Niğde Ömer Halisdemir Üniversitesi Mühendislik Bilimleri Dergisi
Niğde Ömer Halisdemir University Journal of Engineering Sciences

Araştırma makalesi / Research article

www.dergipark.org.tr/tr/pub/ngumuh / www.dergipark.org.tr/en/pub/ngumuh

Paleoenvironmental controls on organic matter accumulation in Lower Cretaceous mudstones: Karabük area (Western Pontides)

Alt Kretase çamurtaşlarında organik madde birikimini kontrol eden paleoortamsal faktörler: Karabük bölgesi (Batı Pontidler)

Zeynep Döner[1,*]

[1] *İstanbul Teknik Üniversitesi, Jeoloji Mühendisliği Bölümü, 34469, İstanbul Türkiye*

Abstract

The lower Cretaceous period marks a global interval of extensive source rock development and significant oil-natural gas accumulation. The aim of this study is to reveal the depositional controls on organic matter enrichment in lower Cretaceous organic-bearing mudstones exposed around the Çukurca–Karabük area (western Pontides). In this study, origin, tectonic setting, paleoclimate, paleosalinity, detrital input, sedimentation rate, paleoproductivity, and paleoredox conditions were assessed. The findings indicate that the mudstones were deposited in the shallow marginal basin-shelf transition zone where brackish-saltwater marine conditions dominated. Semi-humid-semi-arid climate conditions and moderate chemical weathering were effective in deposition. It has been determined that paleoclimate and variable paleoproductivity factors do not play a primary role in organic matter accumulation, episodic oxygen deficiency developing under oxic–suboxic redox conditions contributes to the preservation of organic matter. Fluctuations in sedimentation rate both diluted the organic matter and increased oxidative degradation. However, identifying the dominant mechanisms controlling the organic matter accumulation and trace elements remains challenging due to the simultaneous and complex interaction of different oceanographic processes.

Keywords: Lower Cretaceous mudstones, Organic matter enrichments, Trace elements, Paleoenvironment, Karabük area (western Pontides)

Öz

Alt Kretase dönemi, küresel ölçekte önemli petrol ve doğal gaz rezervlerinin oluştuğu ve kaynak kaya gelişiminin yaygın olduğu bir dönemdir. Bu çalışmanın amacı, Batı Pontidler'de Çukurca-Karabük bölgesi civarında yüzeyleyen alt Kretase yaşlı organik madde içeren çamurtaşlarında organik madde birikimini kontrol eden çökelme ortamı koşullarını ortaya koymaktadır. Çalışmada köken-tektonik ortam, paleoiklim, paleotuzluluk, detritik girdi, sedimantasyon hızı, paleoüretkenlik ve paleoredoks koşulları değerlendirilmiştir. Bulgular, çamurtaşlarının acı su–tuzlu denizel koşulların egemen olduğu sığ kenar havza–şelf geçiş zonunda çökelmiş olduğunu göstermektedir. Çökelmede yarı nemli–yarı kurak iklim koşulları ve orta dereceli kimyasal ayrışma etkili olmuştur. Paleoiklim ve değişken paleoüretkenlik faktörlerinin organik madde birikiminde birincil bir rol oynamadığı, oksik–suboksik redoks koşulları altında gelişen epizodik oksijen eksikliğinin organik madde korunmasına katkı sağladığı belirlenmiştir. Sedimantasyon hızındaki dalgalanmalar organik maddeyi hem seyreltmiş hem de oksidatif bozunmayı artırmıştır. Bununla birlikte, organik madde ve iz elementlerin birikimini kontrol eden baskın mekanizmaların tanımlanması, farklı oşinografik süreçlerin eşzamanlı ve karmaşık etkileşimi nedeniyle güçlüğünü korumaktadır.

Anahtar kelimeler: Alt Kretase çamurtaşları, Organik madde zenginleşmesi, İz elementler, Paleoortam, Karabük bölgesi (batı Pontidler)

1 Introduction

Fine-grained sedimentary rocks preserve the most complete records of Earth's geological history [1–3], and their chemical compositions allow for the reconstruction of paleoenvironmental conditions [3, 4]. Numerous researchers have used the geochemical characteristics of these rocks to determine paleoenvironmental parameters [3, 5, 6]. In the characterization of depositional environments, paleoclimate [7–9], paleosalinity [10], paleoredox conditions [11–14], sea-level fluctuations [3, 15], paleoproductivity [8, 16–21], detrital input, and sedimentation rates [22–25] are commonly employed as key indicators. The accumulation, preservation, and enrichment of organic matter in the source rock are directly linked to depositional environment conditions [8, 19, 25–27], and variations in these environmental conditions play a decisive role in the production, transport, deposition, and organic matter abundance [3, 9, 11, 15, 28, 29]. Moreover, the hydrocarbon potential of source rocks largely depends on their organic matter. Therefore, investigating the depositional factors that control the accumulation, preservation, and enrichment of organic matter is of both theoretical and practical importance for evaluating resource potential and identifying new exploration targets [30–32].

This study focuses on lower Cretaceous organic-bearing mudstones exposed around the Çukurca–Karabük (Türkiye)

* Sorumlu yazar / Corresponding author, e-posta / e-mail: donerz@itu.edu.tr (Z. Döner)
Geliş / Received: 03.11.2025 Kabul / Accepted: 16.12.2025 Yayımlanma / Published: 15.01.2026
doi: 10.28948/ngumuh.1816402

area within the western Pontides. The lower Cretaceous represents a period during which approximately 29% of the world's original recoverable oil and natural gas reserves were formed and corresponds to one of the globally recognized anoxic stratigraphic intervals [33]. Although the sea level was relatively low during the early stages of this period, especially during the Aptian–Albian, which is critical in terms of both the expansion of epicontinental seas and the development of anoxic facies, it rose significantly [34]. Numerous studies around study area have been conducted by researchers on the general geology, sedimentology, and stratigraphy [35–53]. Moreover, several studies have examined the hydrocarbon source rock potential in the vicinity of the study area [42, 54–59]. However, the processes controlling organic matter enrichment in the lower Cretaceous mudstones forming the basis of this study have not yet been fully investigated. Therefore, these units constitute an important regional representative for understanding the characteristic depositional conditions of this period.

The primary objective of this study is to elucidate the depositional environmental conditions that exerted control over the accumulation of organic matter in lower Cretaceous organic-bearing mudstones exposed in the vicinity of the Çukurca–Karabük (western Pontides) region. In this context, the origin and tectonic setting, paleoclimate and weathering, paleoredox conditions, paleosalinity, paleoproductivity, detrital input, and sedimentation rate were evaluated.

A detailed characterization of these parameters in this study will not only shed light on the characteristics of hydrocarbon systems in comparable environments but also provide a scientific foundation for future investigations.

2 Geological setting

The İstanbul–Zonguldak Zone was formed through the amalgamation of pre-Ordovician metamorphic units, island-arc volcanism, and oceanic fragments, and is subsequently characterized by a transgressive Paleozoic succession that developed between the Ordovician and Carboniferous [60, 61]. This succession was deposited on an upper Neoproterozoic granitic and metamorphic basement [62, 63], deformed during the Carboniferous Variscan Orogeny, and is cut by late Permian granites [64–66]. Permo-Triassic sedimentary units unconformably cover this succession [63].

The study area is located within this zone on the Hercynian continental fragment in the northern part of the western Pontides (Figure 1), and the geological evolution of the unit parallels the development of Eurasia beginning in the early Paleozoic [68]. The closure of the Paleo-Tethys Ocean in the Late Jurassic led to the emplacement of the zone onto an ophiolitic sequence; during the Mesozoic, the Pontides were situated along the southern margin of the active continental edge of Laurasia, and in the Late Cretaceous they experienced a tectonic evolution concurrent with their separation from Laurasia and the opening of the oceanic back-arc basin of the Black Sea [63, 69–73].

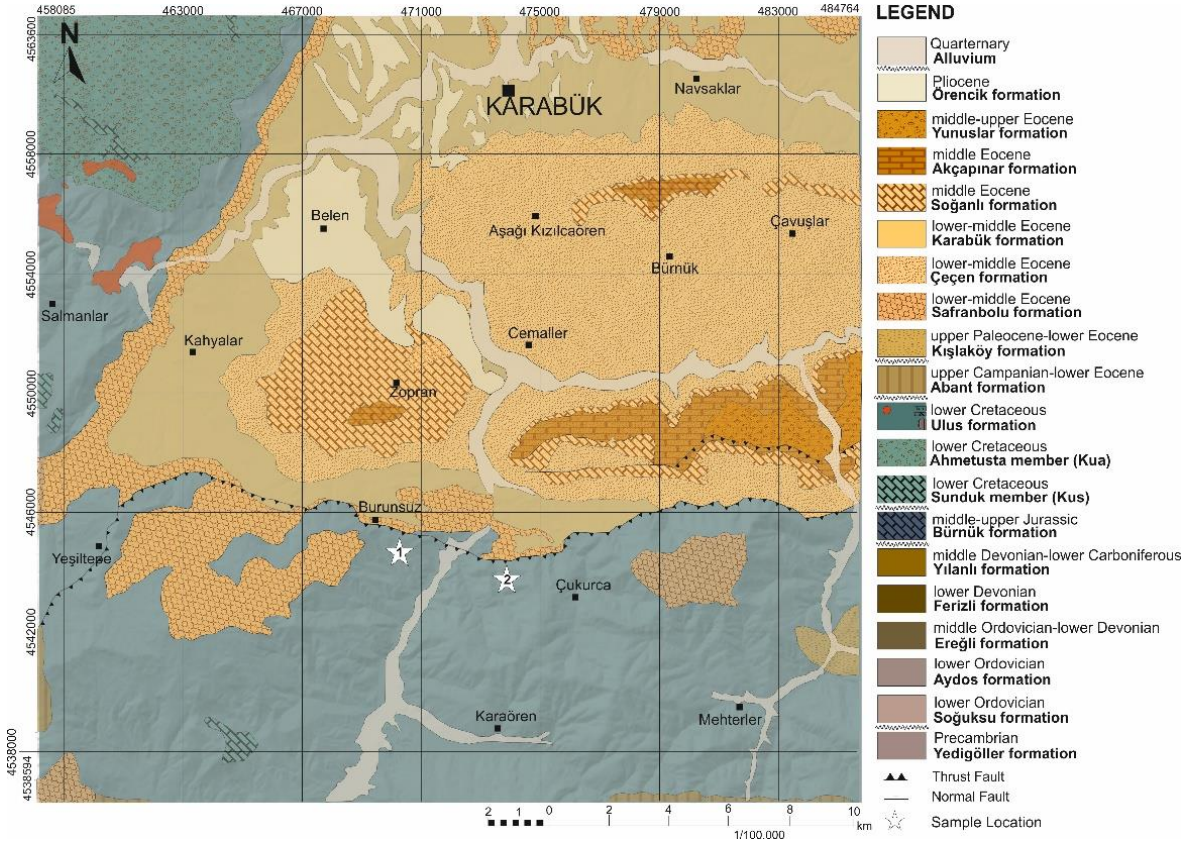

Figure 1. Geological map of the study area (modified from [67])

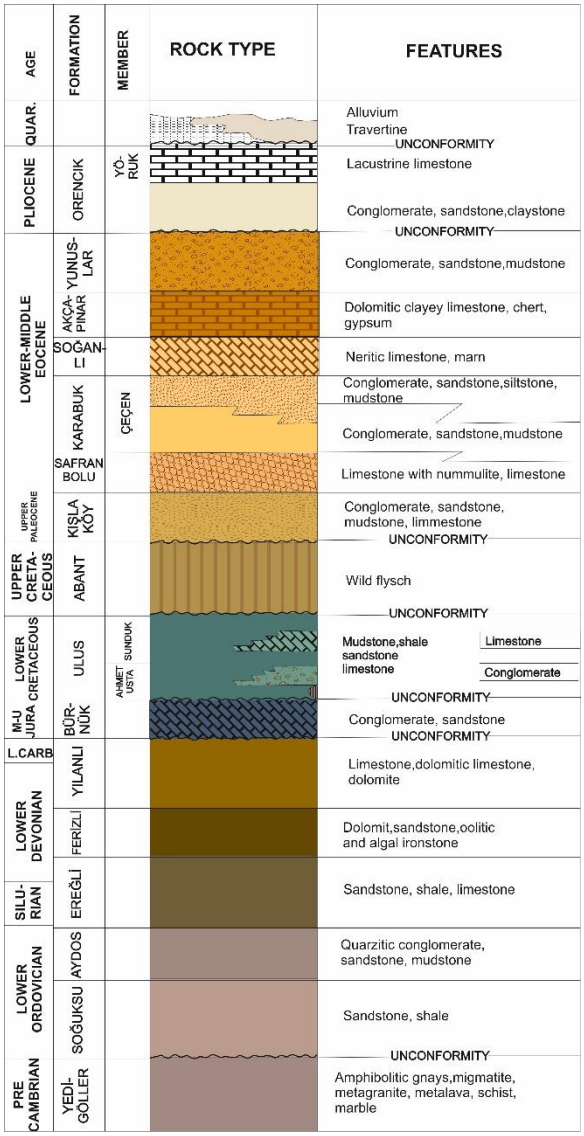

Figure 2. The generalized stratigraphic column section of the study area (modified from [67])

A generalized stratigraphic section of the study area is presented in Figure 2. Accordingly, the lowermost unit is the Precambrian Yedigöller formation, consisting of amphibolite, gneiss, migmatite, metaleucogranite, schist, and marble. This is overlain by the lower Ordovician Soğuksu formation (interbedded shale and sandstone) and the coeval Aydos formation (quartzitic conglomerate, sandstone, and mudstone).

Above these lie the middle Ordovician–lower Devonian Ereğli formation (sandstone, shale, limestone), the lower Devonian Ferizli formation (dolomite, sandstone, oolitic and algal ironstone), and the lower Devonian–lower Carboniferous Yılanlı formation (limestone, dolomitic limestone, dolomite). At higher stratigraphic levels, the Dogger–Malm aged Bürnük formation (conglomerate, sandstone) occurs. Overlying these units is the lower Cretaceous Ulus formation, represented by alternating mudstone, shale, sandstone, and limestone, which in the central Pontides was previously referred to as the Çağlayan formation [74]. Within this formation, conglomerates are assigned to the Ahmetusta member, and limestones to the Sunduk member. The analyzed mudstone samples in this study were collected from this formation. Around the Çukurca-Karabük region, much of the land area is covered, only limited exposures are available. The outcropping mudstone samples examined in this study macroscopically display light to dark gray-greenish-brown color and contain intercalated silt and clay. The samples are fine- to-medium-grained and moderately sorted. Laminations and bedding structures are indistinct (Figure 3). The samples exhibit moderate hardness and brittle behavior, and the presence of calcite veins indicates evidence for diagenetic processes. Interbedded hemipelagic limestones with micritic textures suggest deposition in relatively deeper marine settings with limited siliciclastic supply. The sandstone layers within the formation imply episodes of high-energy conditions, most likely associated with turbidity flows or storm-induced sedimentation.

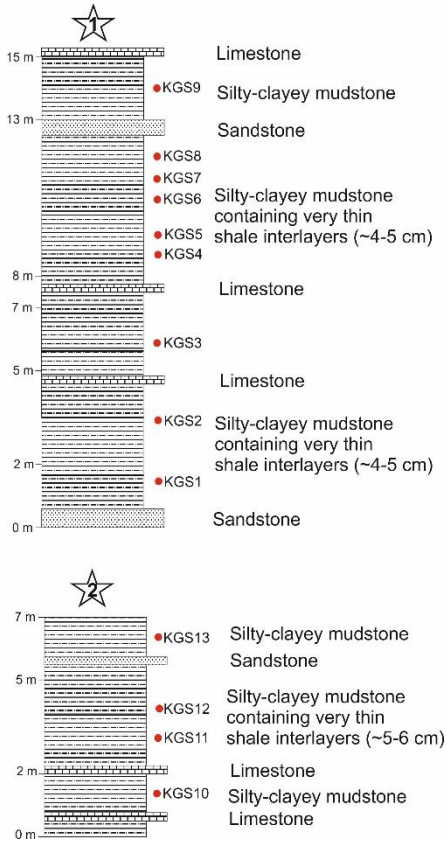

Figure 3. The vertical stratigraphic sections (base-to-top) from two different locations (1 and 2) as shown in the geological map of the study area

This succession is followed by the upper Campanian–Maastrichtian Abant formation (blocky flysch). The upper Danian–Ypresian Kışlaköy formation (conglomerate, sandstone, mudstone, limestone), the lower–middle Eocene Safranbolu formation (Nummulites-bearing, reefal limestone), and the Karabük formation (conglomerate,

sandstone, mudstone), which contains the Cerçen member, overlie this sequence. The stratigraphy continues with the middle Eocene Soğanlı formation (neritic limestone), the Akçapınar formation (dolomitic–argillaceous limestone, chert, gypsum), and the Yunuslar formation (conglomerate, sandstone, mudstone). The uppermost units include the Pliocene Örencik formation (conglomerate, sandstone, claystone), and Quaternary alluvium deposits [67].

3 Materials and methods

In this study, thirteen outcrop mudstone samples from the lower Cretaceous strata were collected from two different locations around Çukurca-Karabük (western Pontides), with nine samples from the first location and four from the second. All collected mudstone samples were subjected to whole-rock geochemical analyses. The major oxides, together with the total organic carbon (TOC) and total sulfur (TS) values, trace elements, rare earth elements (REEs) results, and the calculated paleoenvironment proxies are presented in Tables 1, 2, 3, and 4.

Major oxide analyses were carried out using an X-ray fluorescence spectrometer (XRF; Bruker S8 Tiger) within the wavelength range of 0.01-12 nm. Trace element concentrations were measured by inductively coupled plasma mass spectrometry (ICP-MS; Elan DRC-e-Perkin Elmer). For trace element analysis, approximately 50 mg of powdered sample underwent a two-stage acid digestion procedure. In the first stage, a mixture of HCl (6 mL, 37%), HNO_3 (2 mL, 65%), and HF (1 mL, 38–40%) was digested in a Teflon vessel (pressure- and temperature-controlled) at 135 °C using a Berghoff microwave system. Subsequently, 6 mL of 5% boric acid solution was added to the mixture. Analytical precision for both major and trace element analyses is approximately 5%. TS content was determined using a Leco SC 144 DR sulfur/carbon analyzer with an analytical precision >0.1%.

All major, trace, REE, and TS analyses were conducted at the Istanbul Technical University Geochemistry Research Laboratories (ITU/JAL). In addition, Li, Be, Co, Ni, Cu, Zn, Pb, Ag, Se, Sr, and Re concentrations were determined using an inductively coupled plasma optical emission spectrometer (ICP-OES; Optima 7000-Perkin Elmer) at the Istanbul Technical University Environmental Engineering Department. Instrument calibrations for all analyses were performed using certified reference materials (CRMs), internal standards, and blank samples, and the accuracy of the results was ensured through quality control procedures. Besides, the TOC contents were performed by the Rock-Eval VI analyzer following the standard of IFP 160000 (Institut Français du Pétrole) with analytical precision within 3% in the Turkish Petroleum Research and Development Center.

Table 1. Major oxides, TOC, and TS (contents in wt.%), the chemical index of alteration (CIA), and the index of compositional variability (ICV) of the studied mudstones

Major element	KGS1	KGS2	KGS3	KGS4	KGS5	KGS6	KGS7	KGS8	KGS9	KGS10	KGS11	KGS12	KGS13
SiO_2	68.0	69.8	67.5	66.2	56.6	64.0	67.8	67.4	66.9	56.7	66.1	65.7	56.5
Al_2O_3	11.6	14.4	10.2	10.7	7.11	9.68	14.7	10.1	11.5	9.58	10.6	14.3	7.01
Fe_2O_3	4.34	3.96	5.43	6.42	3.14	4.04	4.72	5.42	4.33	4.02	6.40	3.95	3.12
MgO	1.47	1.57	1.52	1.70	0.95	1.20	1.48	1.50	1.45	1.19	1.69	1.55	0.94
CaO	3.71	10.8	4.45	3.31	4.42	7.94	14.0	4.44	3.70	7.93	3.30	10.7	4.40
Na_2O	0.59	0.56	0.39	0.40	0.69	0.32	0.50	0.38	0.58	0.30	0.38	0.54	0.68
K_2O	2.20	2.76	2.26	2.14	2.32	2.28	2.71	2.25	2.19	2.26	2.13	2.75	2.31
TiO_2	0.51	0.77	0.55	0.56	0.45	0.52	0.76	0.54	0.49	0.51	0.55	0.76	0.44
P_2O_5	0.10	0.09	0.11	0.09	0.10	0.11	0.09	0.10	0.08	0.10	0.09	0.09	0.10
MnO	0.02	0.03	0.03	0.04	0.03	0.04	0.04	0.04	0.03	0.04	0.03	0.02	0.03
Cr_2O_3	0.01	0.01	0.01	0.04	0.01	0.01	0.01	0.01	0.02	0.01	0.03	0.01	0.01
K_2O/Al_2O_3	0.19	0.19	0.22	0.20	0.33	0.24	0.18	0.22	0.19	0.24	0.20	0.19	0.33
K_2O/Na_2O	3.73	4.93	5.79	5.35	3.36	7.13	5.42	5.92	3.78	7.53	5.61	5.09	3.40
CIA	72.9	74.9	73.2	74.7	59.8	73.3	76.3	73.3	72.9	73.6	74.9	75.1	59.7
ICV	1.11	1.42	1.43	1.36	1.69	1.69	1.65	1.44	1.11	1.70	1.37	1.41	1.70
TOC	0.58	0.48	0.66	0.62	0.59	0.62	0.64	0.52	0.42	0.60	0.56	0.53	0.56
TS	0.02	0.03	0.02	0.01	0.02	0.01	0.03	0.01	0.02	0.03	0.02	0.02	0.01

Table 2. Trace element contents of the studied mudstones (contents in ppm, except for Au in ppb)

Trace element	KGS1	KGS2	KGS3	KGS4	KGS5	KGS6	KGS7	KGS8	KGS9	KGS10	KGS11	KGS12	KGS13
Sc	12.5	13.7	13.8	15.6	12.1	15.6	12.8	11.9	17.5	13.4	15.8	12.1	14.6
Y	10.0	14.1	12.7	16.4	11.6	12.0	15.8	16.5	10.1	14.2	12.5	11.8	12.1
Th	27.1	28.9	27.3	28.5	24.9	26.5	29.2	28.6	27.1	28.9	27.4	24.9	26.6
Li	55.3	53.1	65.3	58.8	46.9	58.6	60.4	58.9	55.4	53.2	65.5	46.8	58.7
Be	0.00	0.00	0.00	0.00	0.00	0.00	0.00	0.00	0.00	0.00	0.00	0.00	0.00
Co	11.5	28.3	13.4	19.8	11.7	39.1	37.9	15.0	11.0	18.3	13.0	11.8	19.1
Ni	33.5	57.5	55.7	30.4	21.0	32.4	35.4	30.5	33.6	57.6	35.6	21.1	32.3
Cu	40.5	35.5	29.5	35.3	45.9	24.9	25.1	35.4	50.4	55.6	39.4	45.7	35.0
Zn	84.2	95.6	81.9	112.2	82.1	92.6	229.2	112.3	84.3	95.7	82.0	82.2	92.7
Ga	16.1	16.2	24.0	18.3	22.2	23.4	24.3	18.4	16.2	16.3	14.1	22.3	23.5
As	10.3	48.0	10.0	2.56	9.53	27.6	9.51	2.59	10.4	48.2	10.1	9.56	27.7
Se	0.00	0.00	0.00	0.00	0.00	0.00	0.00	0.00	0.00	0.00	0.00	0.00	0.00
Rb	76.5	94.9	89.9	91.6	69.9	91.9	98.7	91.6	76.4	95.0	90.1	69.9	92.0
Sr	148.6	121.3	132.0	141.6	129.4	169.2	165.5	140.6	147.5	120.1	132.0	160.1	170.1
Ag	0.00	0.00	0.00	0.00	0.00	0.00	0.00	0.00	0.00	0.00	0.00	0.00	0.00
Cd	0.53	0.21	0.13	0.11	0.16	0.10	0.50	0.12	0.57	0.45	0.16	0.19	0.13
In	0.04	0.00	0.03	0.02	0.02	0.01	0.00	0.05	0.07	0.03	0.06	0.05	0.04
Cs	4.11	6.36	4.75	5.80	2.46	4.95	6.67	5.83	4.14	6.39	4.78	2.49	4.98
Ba	427.1	277.9	244.7	548.3	568.9	425.1	173.7	548.4	427.2	278.9	245.8	570.1	426.1
Tl	0.49	0.55	0.37	0.45	0.41	0.47	0.56	0.48	0.52	0.58	0.40	0.44	0.50
Pb	20.9	18.4	68.5	23.8	21.6	25.1	27.6	23.9	21.0	18.6	68.6	21.6	25.2
U	1.70	1.46	2.62	2.12	1.69	2.48	2.59	1.46	1.43	1.46	2.09	1.66	1.73
Au; ppb	0.02	0.03	0.02	0.03	0.04	0.02	0.03	0.03	0.02	0.03	0.02	0.04	0.02
Hf	1.57	2.36	1.84	2.05	1.71	1.59	2.54	2.08	1.60	2.39	1.87	1.74	1.62
Ir	ND	ND	0.00	ND	0.01	ND	0.00	ND	ND	ND	0.03	0.04	ND
Pd	0.13	0.08	0.10	0.09	0.09	0.12	0.08	0.12	0.16	0.11	0.13	0.12	0.15
Pt	0.01	0.01	0.02	0.03	0.02	0.01	0.02	0.06	0.04	0.04	0.05	0.05	0.04
Rh	0.24	0.07	0.11	0.12	0.22	0.11	0.05	0.15	0.27	0.10	0.14	0.25	0.14
Ru	ND	ND	ND	ND	ND	ND	ND	ND	ND	ND	ND	ND	ND
Sb	0.34	0.41	0.59	0.43	0.37	0.33	0.47	0.46	0.37	0.44	0.62	0.40	0.36
Sn	1.08	1.61	1.29	1.46	0.87	1.17	1.61	1.49	1.11	1.64	1.32	0.90	1.20
Te	ND	ND	ND	ND	ND	ND	ND	ND	ND	ND	ND	ND	ND
V	152.0	152.0	224.0	223.9	150.0	282.6	283.2	129.3	125.0	183.2	156.4	168.9	169.0
Nb	8.43	15.6	9.58	0.84	8.37	10.2	12.5	0.87	8.46	15.7	9.61	8.40	10.2
Mo	0.41	0.63	4.53	0.98	0.88	1.01	4.50	0.48	0.67	0.91	0.44	0.66	0.51
Mn	154.9	232.3	232.3	309.8	232.3	309.8	309.8	154.9	77.4	309.8	232.3	154.9	232.3
Ta	ND	ND	ND	ND	ND	ND	ND	ND	ND	ND	ND	ND	ND
Re	0.00	0.00	0.00	0.00	0.00	0.00	0.00	0.00	0.00	0.00	0.00	0.00	0.00
Zr	51.5	55.6	52.2	56.8	64.7	66.5	76.8	74.8	58.7	56.5	68.8	98.3	92.5

Table 3. REEs contents (in ppm) and calculated systematics of the studied mudstones

	REE	KGS1	KGS2	KGS3	KGS4	KGS5	KGS6	KGS7	KGS8	KGS9	KGS10	KGS11	KGS12	KGS13
	La	48.6	56.2	47.8	50.8	45.0	58.3	66.4	50.6	48.9	55.9	48.0	45.3	58.1
	Ce	32.0	51.1	30.6	35.6	27.0	29.2	51.1	35.4	32.3	50.8	30.8	27.3	39.0
	Pr	4.02	6.02	4.37	5.15	3.54	4.25	6.04	4.95	4.32	5.72	4.57	3.84	4.05
	Nd	14.4	23.1	17.4	21.2	14.0	16.5	22.4	21.0	14.7	22.8	17.6	14.3	16.3
	Sm	2.84	4.37	3.23	4.18	3.52	3.40	4.32	3.98	3.14	4.07	3.43	3.82	3.20
	Eu	0.80	0.94	0.89	0.94	1.06	0.79	0.84	0.74	1.10	0.64	1.09	0.94	0.69
	Gd	2.38	3.67	2.44	3.33	2.62	2.68	3.89	3.13	2.68	3.37	2.64	2.92	2.48
	Tb	0.40	0.41	0.38	0.52	0.34	0.41	0.62	0.32	0.70	0.41	0.58	0.64	0.51
	Dy	2.04	2.91	2.42	3.06	2.28	2.24	3.25	2.86	2.34	2.61	2.62	2.58	2.04
	Ho	0.38	0.60	0.47	0.63	0.43	0.43	0.62	0.43	0.68	0.40	0.67	0.63	0.43
	Er	1.32	2.01	1.54	1.87	1.49	1.31	1.96	1.67	1.62	1.71	1.74	1.79	1.31
	Tm	0.20	0.24	0.24	0.25	0.22	0.26	0.22	0.15	0.25	0.16	0.24	0.22	0.16
	Yb	1.39	1.67	1.64	1.73	3.38	1.33	1.81	1.53	2.69	1.37	1.64	3.68	1.43
	Lu	0.22	0.28	0.30	0.29	0.19	0.20	0.30	0.19	0.22	0.20	0.30	0.29	0.22
REE systematics	ΣREE	111.0	153.5	113.8	129.5	105.1	121.3	163.7	126.9	115.7	150.1	115.9	108.3	129.9
	ΣLREE	102.7	141.7	104.3	117.8	94.1	112.4	151.0	116.6	104.5	139.9	105.5	95.5	121.3
	ΣHREE	8.34	11.8	9.44	11.7	10.94	8.86	12.7	10.3	11.2	10.2	10.4	12.7	8.58
	LREE/HREE	12.3	12.0	11.0	10.1	8.6	12.7	11.9	11.3	9.3	13.7	10.1	7.5	14.1
	$(La/Yb)_{NASC}$	3.43	3.31	2.86	2.89	1.31	4.30	3.61	3.26	1.79	4.01	2.88	1.21	4.00
	Eu/Eu*	0.94	0.71	0.96	0.77	1.07	0.80	0.62	0.64	1.16	0.53	1.10	0.86	0.75

Table 4. The calculated paleoenvironment proxies of the studied mudstones

	Parameters	KGS1	KGS2	KGS3	KGS4	KGS5	KGS6	KGS7	KGS8	KGS9	KGS10	KGS11	KGS12	KGS13
Origin	Zr/Sc	4.10	4.05	3.78	3.64	5.36	4.25	6.00	6.29	3.35	4.22	4.36	8.15	6.32
	Th/Sc	2.16	2.10	1.98	1.83	2.06	1.70	2.28	2.40	1.55	2.16	1.73	2.06	1.82
Paleoclimate	Sr/Cu	3.67	3.42	4.48	4.01	2.82	6.79	6.59	3.98	2.93	2.16	3.35	3.50	4.87
	Rb/Sr	0.51	0.78	0.68	0.65	0.54	0.54	0.60	0.65	0.52	0.79	0.68	0.44	0.54
	Ga/Rb	0.21	0.17	0.27	0.20	0.32	0.25	0.25	0.20	0.21	0.17	0.16	0.32	0.26
	C-value	0.52	0.25	0.61	0.82	0.36	0.33	0.25	0.61	0.53	0.34	0.83	0.25	0.36
Paleoredox	V/Cr	2.22	2.22	3.27	0.82	2.19	4.13	4.14	1.89	0.91	2.68	0.76	2.47	2.47
	Th/U	15.9	19.8	10.4	13.5	14.7	10.7	11.3	19.6	18.9	19.7	13.1	15.0	15.4
	C_{org}/P	34.3	31.6	35.5	40.8	34.9	33.4	42.1	30.8	31.1	35.5	36.8	34.9	33.1
	Mo_{EF}	0.04	0.06	0.45	0.10	0.09	0.45	0.10	0.05	0.07	0.09	0.04	0.07	0.05
	U_{EF}	0.50	0.43	0.78	0.63	0.50	0.74	0.77	0.43	0.42	0.43	0.62	0.49	0.51
Paleo salinity	Sr/Ba	0.35	0.44	0.54	0.26	0.23	0.40	0.95	0.26	0.35	0.43	0.54	0.28	0.40
	Rb/K	0.004	0.004	0.005	0.005	0.004	0.005	0.004	0.005	0.004	0.005	0.005	0.003	0.005
	CaO/CaO+Fe	0.55	0.80	0.54	0.42	0.67	0.74	0.81	0.54	0.55	0.74	0.42	0.79	0.67
Paleoproductivity	P/Al	0.007	0.005	0.009	0.007	0.012	0.009	0.003	0.008	0.006	0.009	0.007	0.005	0.012
	Cu/Al	0.0007	0.0005	0.0005	0.0006	0.0012	0.0005	0.0003	0.0007	0.0008	0.0011	0.0007	0.0006	0.0009
	Ni/Al	0.0005	0.0008	0.0010	0.0005	0.0006	0.0006	0.0005	0.0006	0.0006	0.0011	0.0006	0.0003	0.0009
	Ba/Al	0.007	0.004	0.005	0.010	0.015	0.008	0.002	0.010	0.007	0.006	0.004	0.008	0.011
	Ba_{bio}	427.1	277.8	244.7	548.3	568.9	425.0	173.7	548.4	427.1	278.8	245.7	570.0	426.1
Detrital input	Si/Al	5.10	3.30	5.84	5.46	9.52	5.84	4.07	5.89	5.14	5.89	5.51	3.32	9.64
	Ti/Al	0.05	0.06	0.06	0.06	0.07	0.06	0.06	0.06	0.05	0.06	0.06	0.06	0.07
	Zr/Al	0.0008	0.0007	0.0010	0.0010	0.0017	0.0013	0.0010	0.0014	0.0010	0.0011	0.0012	0.0013	0.0025
	Nb/Al	0.0001	0.0002	0.0002	0.0000	0.0002	0.0002	0.0002	0.0000	0.0001	0.0003	0.0002	0.0001	0.0003
	Th/Al	0.0004	0.0004	0.0005	0.0005	0.0007	0.0005	0.0004	0.0005	0.0004	0.0006	0.0005	0.0003	0.0007

4 Results and discussion

4.1 Origin and tectonic setting

The provenance of mudstones is a critical factor in the evaluation of oil-natural gas basins, as it influences source-rock potential [25]. Tectonic setting exerts a significant influence on the origin of sedimentary rocks. The provenance, tectonic setting, and degree of weathering of clastic sediments can be inferred from their geochemical composition [75–77]. In this study, the SiO_2–Log(K_2O/Na_2O) diagram [5] and La–Th–Sc tectonic discrimination diagram [29] were utilized. Based on the positions of the studied samples in these diagrams, the samples plot within the passive continental margin field on the SiO_2–Log(K_2O/Na_2O) diagram [5], whereas on the La–Th–Sc ternary diagram [29] they fall within both passive and active continental margin fields (Figure 4 a,b).

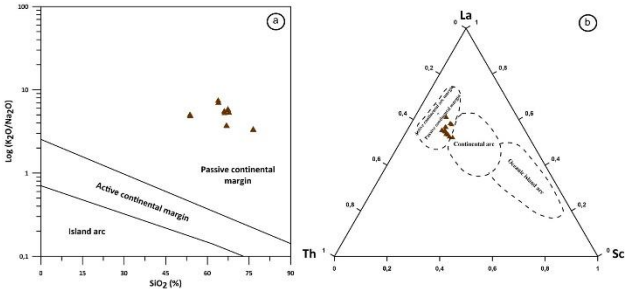

Figure 4. The tectonic classification diagrams; a) SiO_2 vs. Log (K_2O/Na_2O) [5], b) La–Th–Sc [29]

This indicates a possible influence of volcanic or continental arc sources on the sediment supply [76], supporting previous studies suggesting that the Black Sea region was influenced by continental arc activity throughout the Cretaceous [66]. In addition, Zr/Sc–Th/Sc diagram [78] (Figure 5a) and Zr–TiO_2 binary plots [79] (Figure 5b) were employed. The positions of the samples on these diagrams indicate that the studied mudstones were predominantly derived from an intermediate-composition magmatic source and that sedimentary recycling did not occur.

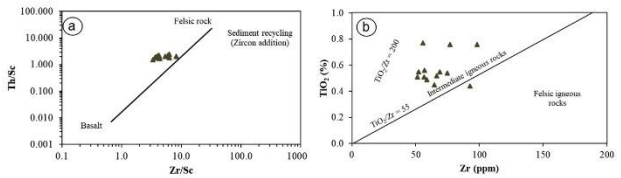

Figure 5. The plots of a) Zr/Sc vs. Th/Sc [78], b) Zr vs. TiO_2 [79]

Felsic rocks are typically characterized by high ratios of LREE/HREE and weak Eu anomalies, whereas mafic rocks exhibit low ratios of LREE/HREE and pronounced Eu anomalies [4]. The LREE enrichment and moderate Eu anomaly observed in the analyzed samples (Eu/Eu* = 0.53-1.16; avg. 0.84; Table 3) predominantly reflect an intermediate-composition source, marking a transition from a passive to an active continental margin setting.

4.2 Factors controlling the organic matter accumulation

4.2.1 Paleoclimate and weathering

Paleoclimatic conditions influence exogenic processes and thus control the development of sedimentary environments. The distribution, ratios, and relative concentrations of trace elements can be used as indicators for reconstructing paleoclimatic variations [25]. Among these, Sr/Cu and Rb/Sr ratios are widely employed as paleoclimatic proxies [80, 81]. Sr element tends to exhibit higher values under hot and arid conditions, whereas Cu element, being less mobile in aqueous environments, displays lower values in sediments. Accordingly, Sr/Cu ratios ranging between 1.3 and 5 indicate warm and humid paleoclimatic conditions, whereas values greater than 5 reflect hot and arid climates [25, 82]. In addition, the Rb/Sr ratio can also be used as a paleoclimatic indicator, where low values correspond to warm climates and high values indicate cold climatic conditions [83]. The Sr/Cu and Rb/Sr ratios of the analyzed mudstones range from 2.16 to 6.79 (avg. 4.04) and from 0.44 to 0.79 (avg. 0.61), respectively (Table 4). Based on the Sr/Cu and Rb/Sr values, together with the positions of the samples on the K_2O/Al_2O_3–Ga/Rb and Sr/Cu–Ga/Rb diagrams [84] (Figure 6a,b), it can be inferred that a transition from warm–humid to semi-arid climatic conditions prevailed during the deposition of the mudstones. Additionally, the C-value [Σ(Fe + Mn + Cr + Ni + V + Co) / Σ(Ca + Mg + Na + Sr + Ba + K)] is also used as a paleoclimatic indicator, where C-values >0.8 indicate humid paleoclimate, 0.6 - 0.8 semi-humid climate, 0.4 - 0.6 semi-arid to semi-humid climate, 0.2 - 0.4 semi-arid climate, and <0.2 arid climate [85]. The C-values of the studied samples range between 0.25 and 0.83, with an average value of 0.47 (Table 4), indicating semi-arid to semi-humid paleoclimatic conditions, which is consistent with the results obtained from ratios of Sr/Cu and Rb/Sr and the binary diagrams (Figure 6a,b).

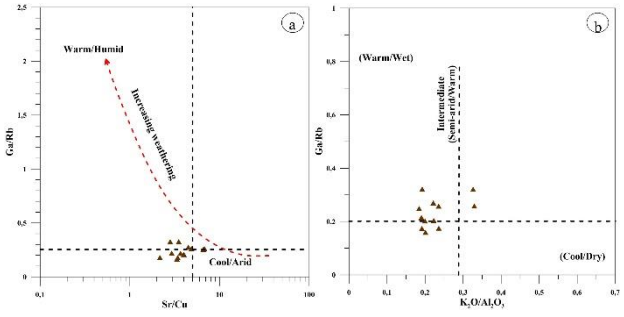

Figure 6. Paleoclimate discrimination diagrams; a) Sr/Cu vs. Ga/Rb [84], b) K_2O/Al_2O_3 vs. Ga/Rb [84]

The chemical weathering degree and paleoclimatic conditions in the source areas can be determined using the Chemical Index of Alteration (CIA). The CIA is calculated on a molar basis as [Al_2O_3 / (Al_2O_3 + CaO* + Na_2O + K_2O)] × 100 [86, 87], where the corrected CaO* value for silicate minerals follows the method proposed by [78]. CIA values between 50 and 65 indicate low degrees of chemical weathering under cold and arid climatic conditions; values

between 65 and 85 indicate moderate weathering under warm and humid climates; and values between 85 and 100 reflect intense chemical weathering under warm and humid conditions [87–89]. During chemical weathering, immobile cations such as Al^{3+} and Ti^{4+} are retained, whereas mobile cations such as Na^{+} and Ca^{2+} are leached out [4, 90]. Large-ion radius cations (e.g., Al, Mg, Cs) remain relatively stable, while smaller ions (e.g., Ca, Na, K) tend to dissolve and be removed; hence, element abundances depend on the intensity of weathering [87, 91–93]. The CIA values of the analyzed samples range from 59.7 to 76.3, with an average of 71.9 (Table 1). These values fall within the range of 65 - 85 [87–89], are higher than those of the Upper Continental Crust (UCC, CIA = 56.9; [94]) and Post-Archean Average Australian Shale (PAAS, CIA = 69.0; [91]), and indicate moderate chemical weathering under semi-arid to warm-humid paleoclimatic conditions. In addition, the compositional variability index (ICV = (Fe_2O_3 + K_2O + Na_2O + CaO + MgO + MnO + TiO_2) / Al_2O_3) is widely applied to estimate the initial composition of sediments and to determine the degree of sedimentary recycling [95–97]. An ICV value > 1 indicates first-cycle deposition, whereas ICV < 1 suggests that the sediments may have undergone significant chemical weathering or sedimentary recycling [95, 97]. The ICV values of the studied samples are greater than 1 (ranging from 1.11 to 1.70, with an average of 1.47; Table 1), indicating that sedimentary recycling did not significantly affect their composition. Additionally, the low Zr/Sc ratios (< 25; [78]) further support first-cycle deposition of the studied sediments.

The A–CN–K (Al_2O_3 – CaO*+Na_2O – K_2O) ternary diagram is commonly used to distinguish between compositional variations related to chemical weathering and those related to source-rock composition. Although highly weathered products typically display CIA values aligned along a straight trend parallel to the A–CN edge (representing the ideal weathering trend) [87, 98], most of the data from the studied samples deviate from this theoretical trend, indicating K_2O addition due to diagenetic K-metasomatism [90, 97, 98] (Figure 7).

Since K-metasomatism can lower CIA values by introducing K^{+}, a correction is required to remove the influence of illitization [96–98]. Application of the corrected CIA formula (CIA_{corr} = [Al_2O_3 / (Al_2O_3 + CaO* + Na_2O + K_2O_{corr})] × 100) to the studied samples yields CIA_{corr} values ranging between 69.6 and 81.0 (avg. 78.2). Although these values show only minor differences from the original CIA values, they still fall within the intermediate range and indicate warm–humid climatic conditions. Therefore, the CIA index can be regarded as a reliable indicator for assessing weathering intensity and paleoclimatic conditions. Furthermore, extension of the linear trend parallel to the A–CN edge on the ternary plot suggests that the source rocks were close to granite and granodiorite composition, which is also supported by the provenance diagrams (Figure 7).

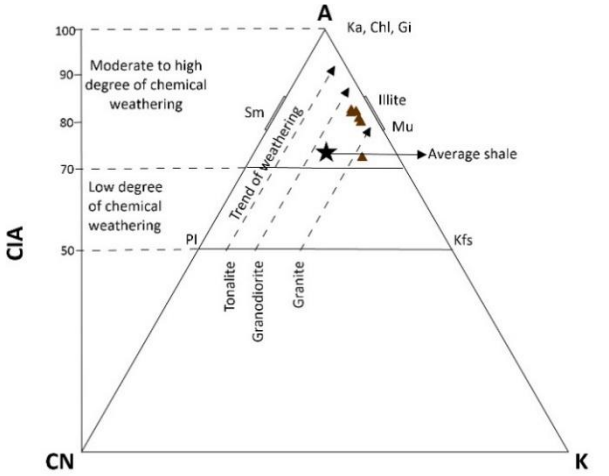

Figure 7. The A-CN-K (Al_2O_3 - CaO* + Na_2O - K_2O) ternary diagrams, along with corresponding changes in the chemical index of alteration (CIA) [99]. Abbreviations: Ka; kaolinite, Chl; chlorite, Gi; gibbsite, Sm; smectite, Mu; muscovite, Pl; plagioclase, Kfs-K; feldspar

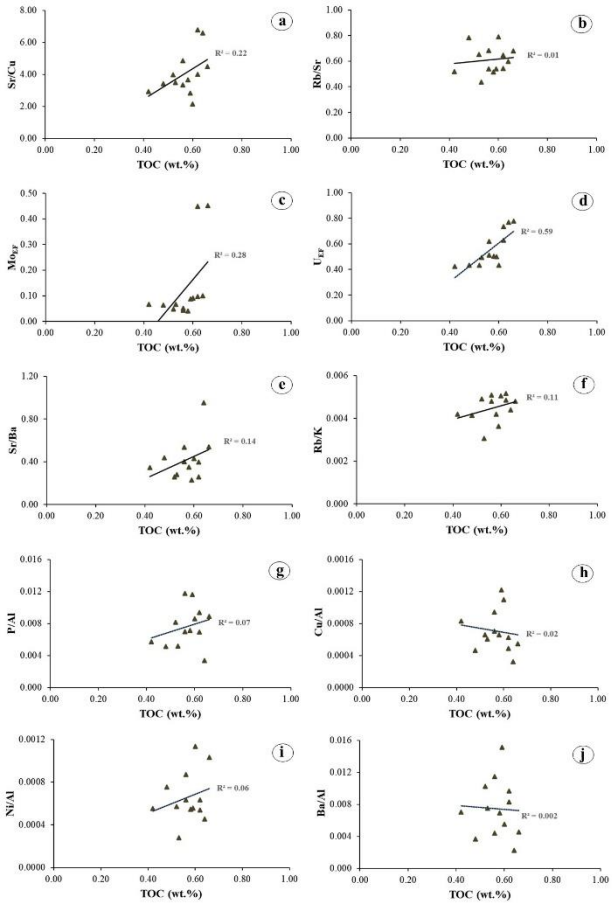

Figure 8. The bivariate plots of TOC vs. paleoclimate (a, b), paleoredox (c-d), paleosalinity (e-f), and paleoproductivity (g-h-i-j) proxies

The paleoclimatic variations play an indirect role in the organic matter' accumulation and preservation, influencing sediment input and water-column stratification. These conditions limit both the diversity and abundance of biological communities within the water masses [88]. Temperate and humid climatic conditions promote organism growth and enhance organic matter production compared to hot and arid climates [25, 100]. The lack of correlation between the paleoclimatic indicators (Sr/Cu and Rb/Sr) and TOC (Figure 8a,b) suggests that paleoclimatic conditions may not have played a significant role in organic carbon enrichment.

The geochemical and mineralogical characteristics of sedimentary rocks are influenced by the chemical weathering degree in the source area [27]. Climatic conditions not only control the chemical weathering intensity [4, 101] but also influence the conditions governing organic matter enrichment [10, 19]. Based on CIA values (avg. 71.9) and the position of the samples on the A–CN–K diagram (Figure 7), the studied mudstones experienced moderate chemical weathering. Although the CIA index is widely used to evaluate the degree of chemical weathering, caution is required when directly linking it to paleoclimate because non-weathering factors such as origin, sedimentary recycling, and diagenetic processes may also influence the values [97]. Elevated CIA values may result from sedimentary recycling processes that increase clay mineral content. Therefore, additional proxies, ICV and Zr/Sc ratios, were also employed in this study. The high ICV values (avg. 1.47; Table 1) and low Zr/Sc ratios (avg. 4.91; Table 4) indicate that the studied samples did not undergo significant sediment recycling and are consistent with a first-cycle sediment origin.

4.2.2 Paleoredox condition

Redox conditions, based on dissolved oxygen concentrations (mL O_2/L H_2O), can be classified as oxic ($[O_2] > 2$), suboxic ($2 > [O_2] > 0.2$), anoxic ($[O_2] < 0.2$; no free H_2S in the water column), and euxinic ($[O_2] = 0$; free H_2S present in the water column) [28, 30, 102, 103]. The redox state of the water column controls the solubility, preservation, and oxidation states of redox-sensitive elements such as Mo, U, V, Zn, Ni, and Co, which are widely used as proxies to infer redox conditions in sedimentary environments [12, 27, 104–106]. In this study, considering the relatively low TOC (0.42 - 0.66, avg. 0.57 wt.%) and TS (avg. 0.02 wt.%) values of the mudstones, it can be inferred that oxidizing conditions likely prevailed, and thus redox proxies considered reliable under oxic-suboxic settings can be prioritized. Accordingly, V/Cr and Th/U ratios, trace-element enrichment factors (Mo_{EF} and U_{EF}), and the C_{org}/P ratio were used in this assessment (Table 4).

Although recent studies emphasize that universally applicable elemental thresholds for all systems do not exist [103, 107], earlier research proposed several diagnostic standards. Generally, Th/U > 2 and V/Cr < 4.25 indicate oxic–suboxic conditions, whereas Th/U < 2 and V/Cr > 4.25 are typically associated with anoxic environments [104, 108, 109]. In the studied mudstones, Th/U and V/Cr ratios range from 11.0 to 18.9 and 0.47 to 4.14, respectively, indicating oxic–suboxic conditions. Mo concentrations <25 ppm generally suggest non-euxinic conditions, 25 - 100 ppm indicate euxinic conditions, and >100 ppm reflect strongly euxinic environments [110]. The Mo contents of the studied samples range from 0.41 to 4.53 ppm (avg. 1.28 ppm), all below 25 ppm, supporting non-euxinic conditions. Moreover, Mo_{EF} (avg. 0.13) and U_{EF} (avg. 0.56) values are below the thresholds reported for the California Margin (<2 and <5, respectively), consistent with oxic–suboxic conditions [27, 103, 111, 112]. Additionally, the molar C_{org}/P ratio is widely used to infer redox conditions in marine and lacustrine sediments [113]. C_{org}/P values <50 are typically associated with oxic conditions, whereas values >100 indicate anoxic settings [103, 114, 115]. The C_{org}/P values of the studied samples range from 30.8 to 42.1 (avg. 35.0), supporting oxic conditions and corroborating the other redox proxies.

Changes in paleoredox conditions within the depositional environment directly control the accumulation of organic matter [15, 99, 106]. Recent studies have emphasized that the reliability of redox proxies may vary among formations; therefore, their interpretation should rely on multiple parameters and comprehensive phase-distribution assessments. Moreover, threshold values defined for one formation should not be directly applied to formations of different ages, depositional settings, or redox regimes [103, 107]. Although bimetal ratios (e.g., Ni/Co, V/(V+Ni), V/Sc, Mo/Mn, Cu/Zn) were widely used in earlier studies, they are now considered less reliable because both elements in each ratio are partially redox-sensitive and variably distributed among different sedimentary phases (organic matter, clay minerals, pyrite, etc.), which may prevent them from consistently reflecting redox signals. Instead, enrichment factors are recommended as more robust indicators [27, 107]. In this study, V/Cr, Th/U, and C_{org}/P ratios, along with Mo_{EF} and U_{EF} enrichment factors were used to determine the depositional environments' redox conditions, which were interpreted as oxic–suboxic. Such conditions negatively affected the organic matter preservation. Additionally, the weak ($R^2 = 0.28$) and moderate ($R^2 = 0.59$) correlations between TOC and Mo_{EF} and U_{EF}, respectively (Figure 8c,d), suggest that organic matter underwent aerobic degradation during burial [27, 116].

Under oxic conditions, V, Mo, and U occur in their high-valence, water-soluble forms (V^{5+}, Mo^{6+}, U^{6+}), making them more mobile in the water column. In contrast, under reducing conditions, these elements are converted to their lower-valence forms (V^{3+}, Mo^{4+}, U^{4+}), which promotes their accumulation and retention in sediments [12, 99]. In this context, the weaker correlation between TOC and Mo_{EF} compared to U_{EF} can be attributed to the fact that Mo enrichment typically requires strongly euxinic conditions with free H_2S, whereas U enrichment can occur under a broader range of suboxic to anoxic conditions. This supports the interpretation that suboxic rather than fully euxinic conditions prevailed in the depositional

environment; favorable for U accumulation but insufficient for significant Mo retention [12, 28]. Moreover, variations in oxygen levels within the water column lead to differing geochemical behaviors of Th and U. Under oxic conditions, U remains in the soluble U^{6+} form, while Th occurs as insoluble Th^{4+}; under reducing conditions, Th remains stable, but U is reduced to insoluble U^{4+}. Consequently, low Th/U ratios indicate reducing environments, whereas high ratios reflect oxidizing conditions [109]. In addition, high V/Cr ratios indicate decreasing oxygen levels [99, 104, 109]. Cr element, however, is primarily of detrital origin and is generally unaffected by redox conditions [117].

Although weathering in organic-rich rocks, especially affecting the mobility and redistribution of trace elements associated with organic matter and sulfur phases, may alter absolute concentrations, relative stability of paleoredox proxies can be preserved when weathering intensity is limited [118]. Therefore, when interpreting data obtained from surface samples, both the degree of weathering and the preservation of organic matter should be considered. In this study, moderate weathering conditions prevailed, and the ratio-based proxies used (e.g., V/Cr, Th/U) as well as elemental enrichment factors (e.g., U_{EF}, Mo_{EF}) can be regarded as largely retaining their interpretive reliability. Additionally, variability in elemental concentrations and certain inconsistent relationships in the study area may reflect fluctuations in oxygenation–reduction conditions.

4.2.3 Paleosalinity

Paleosalinity plays a key role in the organic matter preservation and in reconstructing past environmental conditions [25]. Sr and Ba are commonly used as paleosalinity indicators due to their contrasting geochemical behavior: under low-salinity conditions, Ba precipitates as $BaSO_4$ while Sr remains in solution; thus, Sr/Ba ratios increase with rising salinity [81, 119, 120]. The Sr/Ba ratio typically has values <0.2 in freshwater settings, 0.2–0.5 in brackish conditions, and >0.5 in saline marine environments [27, 121]. The Sr/Ba values of the examined mudstones range from 0.23 to 0.95, with an average of 0.43, indicating deposition under brackish to saline marine conditions (Table 2). However, caution is required in interpreting this ratio because Sr can also be associated with carbonates, influencing Sr/Ba values [27, 121].

Changes in salinity during deposition (especially in fine-grained sediments such as shales and mudstones) can also be assessed using Rb/K and CaO/(CaO+Fe) ratios [121, 122]. Because clay minerals can adsorb pore-water ions, these proxies, although semi-quantitative, allow differentiation of paleosalinity conditions into freshwater, brackish, and marine environments. Based on previous studies, intermediate Rb/K (40 - 60 $\times 10^{-4}$) and CaO/(CaO+Fe) (0.2-0.5) ratios indicate brackish conditions; low values (<40 $\times 10^{-4}$; <0.2) reflect freshwater; and high values (~60 $\times 10^{-4}$; >0.5) represent marine conditions [27, 122]. The Rb/K ratios of the studied mudstones range from 0.003 to 0.005 (avg. 0.004; Table 4), and their CaO/(CaO+Fe) ratios vary between 0.42 and 0.81 (avg. 0.63; Table 4), supporting deposition under brackish to saline marine environments.

High paleosalinity, together with increased paleodepth and limited hydrodynamic activity, promotes the development of anoxic redox conditions at the bottom of the water column, which in turn exerts a significant influence on the preservation of organisms within sediments [3, 18, 123]. The examined samples were deposited in brackish to saline marine environments; however, the lack of correlation between TOC and the ratios of Rb/K, Sr/Ba, and CaO/(CaO+Fe) (Figure 8e,f) indicates that brackish–saline conditions did not have a significant impact on organic matter preservation.

In addition, the Sr/Ba ratio was not considered in the interpretation because CaO contents in the samples exceeded the 4% threshold [121]. Carbonate-derived Sr can increase whole-rock Sr/Ba ratios, and thus reliable paleosalinity interpretations require the use of carbonate-free clay fractions [124].

4.2.4 Paleoproductivity

Paleoproductivity in marine environments is directly linked to nutrient availability in the water column and supports both the production and preservation of organic matter [88, 105, 113]. Bio-essential elements such as N, P, Ba, Ni, and Cu are widely used as proxies to evaluate paleoproductivity [105, 113, 115, 125]. In this study, the ratios of P/Al, Ni/Al, Cu/Al, and Ba/Al were used. The P/Al, Cu/Al, Ni/Al, and Ba/Al ratios of the analyzed mudstones range from 0.003 to 0.012 (avg. 0.008), 0.0003 to 0.0012 (avg. 0.0007), 0.0003 to 0.0011 (avg. 0.0007), and 0.0022 to 0.0151 (avg. 0.0074), respectively (Table 4). Some values are lower than those of Post-Archean Australian Shale (PAAS; 0.0078, 0.000893, 0.000714, and 0.0065, respectively; [94]), indicating fluctuations from low to high paleoproductivity levels. Additionally, Ba_{bio} values can be used to evaluate primary productivity in the water column. In this study, Ba_{bio} values were calculated using the formula $Ba_{bio} = Ba_{sample} - Al_{sample} \times (Ba/Al)_{PAAS}$ (0.0075). The Ba_{bio} values of the samples range from 173.7 to 570.0 (avg. 397.0; Table 4), consistent with the results inferred from P/Al, Ni/Al, Cu/Al, and Ba/Al ratios.

Ba in sediments is derived primarily from biological sources, benthic organism secretions, submarine hydrothermal inputs, and terrestrial aluminosilicates [30, 126]. Caution is required when using Ba as a productivity indicator [126–128]. In some cases, Ba values may appear artificially low; under anoxic–suboxic conditions, biogenic Ba cannot be preserved in sediments and may be remobilized, resulting in reduced concentrations. Furthermore, under restricted environmental conditions, sulfate reduction by sulfate-reducing bacteria can lead to barite dissolution, lowering Ba_{bio} content. Conversely, the more oxygenated conditions dominant in the study area suggest that sulfate reduction may not have occurred, and Ba was likely retained in sediments without remobilization. P is an essential nutrient for plankton [88], while Ni and Cu occur in organisms and are primarily delivered to sediments associated with organic matter [28, 30]. After deposition,

organic matter may degrade partially or completely; during this process, released Ni and Cu can be preserved in sediments as sulfide minerals [12, 30, 129].

In the studied samples, no significant correlation was observed between TOC and P/Al, Ni/Al, Cu/Al, and Ba/Al ratios (R^2 = 0.07, 0.06, 0.02, and 0.002, respectively; Figure 8g-j). This suggests that paleoproductivity in the water column did not play a dominant role in TOC enrichment. Additionally, fluctuations in productivity may have exerted a dilution effect on organic matter accumulation, limiting enrichment.

4.2.5 Detrital input - sedimentation rate

Si, Ti, Nb, Th, and Zr are considered indicators of terrigenous detrital input and provide important insights into the intensity of clastic influx [10, 112, 130, 131]. Increases in detrital input may be associated with tectonic activity, sea-level fall, paleoclimatic changes, or the combined influence of these processes [132]. Additionally, climatic fluctuations and salinity variations can also affect detrital supply. In the examined samples, Al-normalized Si, Ti, Zr, Nb, and Th ratios were used (Table 4). Variations in these ratios suggest that the depositional environment was influenced by low-to-moderate detrital input, likely controlled by episodic fluvial or eolian activity.

REEs distributions and North American Shale Composite-normalized $(La/Yb)_{NASC}$ ratios are key indicators used to evaluate sedimentation rates in sedimentary basins [88]. Values close to 1 indicate high sedimentation rates, whereas values significantly above or below 1 reflect low sedimentation rates associated with strong REE fractionation. The $(La/Yb)_{NASC}$ ratios of the analyzed samples range from 1.21 to 4.30 (avg. 2.99; Table 3), indicating fluctuating sedimentation rates throughout the depositional period.

Terrigenous detrital input and sedimentation rate are key factors influencing organic matter enrichment [23, 25]. In this study, Si/Al, Zr/Al, Ti/Al, Nb/Al, and Th/Al ratios were used, and the results indicate that the depositional environment was affected by low-to-moderate detrital influx, likely controlled by episodic fluvial or eolian processes. Additionally, increased terrigenous input during deposition can be attributed to factors such as regional uplift and tectonism, sea-level fall during marine regression phases, paleoclimatic changes, or the combined influence of these processes [132]. Moreover, fluctuating paleoclimatic conditions and variations in water-column salinity may also contribute to changes in detrital supply.

In environments with high sedimentation rates, sediments accumulate rapidly, limiting the interaction time between REEs and seawater, which results in weak REE fractionation; in contrast, low sedimentation rates lead to enhanced fractionation [88, 133]. The variable $(La/Yb)_{NASC}$ values observed in the studied mudstones (1.21-4.30; avg. 2.99) indicate fluctuating sedimentation rates throughout deposition. Low sedimentation rates promote oxidative degradation of organic matter, whereas high sedimentation rates hinder its preservation due to dilution effects. This is consistent with REE adsorption behavior; rapid burial restricts sediment–seawater interaction, thereby limiting REE fractionation [88, 133]. Additionally, there is no distinct similar trend between Al-normalized Si, Ti, Nb, Zr, and Th values and TOC (Figure 9) was observed. This result suggests that variations in detrital input did not exert a dominant control on organic matter accumulation. These findings imply that moderately favorable sedimentation conditions conducive to organic matter preservation did not develop [22].

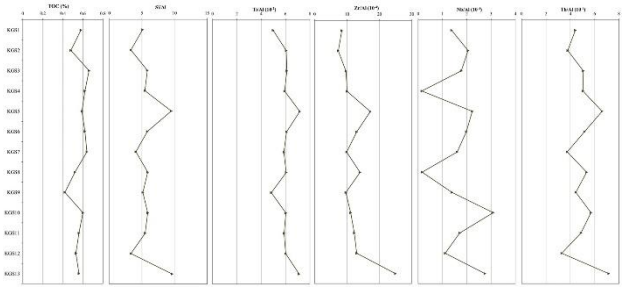

Figure 9. Distribution of detrital input proxies and TOC content of studied mudstones

4.2.6 Depositional model for the studied mudstones

The Cretaceous period is broadly characterized by globally high sea levels, warm climatic conditions, and oceanic anoxic events (OAEs). During this time, extensive and shallow shelf systems developed, promoting efficient organic matter preservation due to increased nutrient supply and reduced oxygenation in ocean waters [33, 134, 135]. However, in the study area, oxic–suboxic redox conditions, a paleoclimate shifting from warm–humid to semi-arid, brackish to saline marine settings, fluctuating paleoproductivity, and variable detrital input and sedimentation rates collectively indicate a depositional setting more consistent with a shelf-margin to shelf-transition zone, rather than a broad passive shelf typical of global Cretaceous trends. Shelf-margin transition zones are characterized by dynamic depositional regimes in which sea-level oscillations, seasonal to mesoscale shifts in the oxygen minimum zone (OMZ) boundary, and detrital dilution may generate complex and heterogeneous paleoenvironmental signals [20, 97, 136]. Accordingly, similar to the study area, such settings may show fluctuating oxygenation between oxic and dysoxic conditions, variable productivity, and limited organic matter preservation when compared to classical continental shelf or deep-marine basin environments [137, 138]. The lack of correlation between TOC and proxies for paleoclimate, salinity, productivity, and detrital input (Figure 8) suggests that these factors did not play a dominant role in organic matter enrichment. Instead, fluctuations in productivity may have had a dilution effect rather than enhancing organic matter accumulation [116, 139], and variable detrital influx together with changing sedimentation rates likely exerted a dual control by promoting oxidative degradation while also diluting organic matter [23–25]. Despite this, paleoredox proxies indicate fluctuating redox conditions within an oxic to suboxic range. Periodic decreases in oxygen availability may have allowed for limited preservation of organic

matter; however, such conditions were insufficient for sustained accumulation.

In summary, the studied mudstones were deposited in a shelf-margin to shelf-transition zone characterized by episodic redox fluctuations, variable productivity, and detrital input, together with fluctuating sedimentation rates. The environment was influenced by hydrodynamic processes capable of reaching the wave base and was governed by multiple controls, including depositional and diagenetic processes as well as climatic and provenance-related factors. Accordingly, a schematic section of the depositional environment model was constructed (Figure 10).

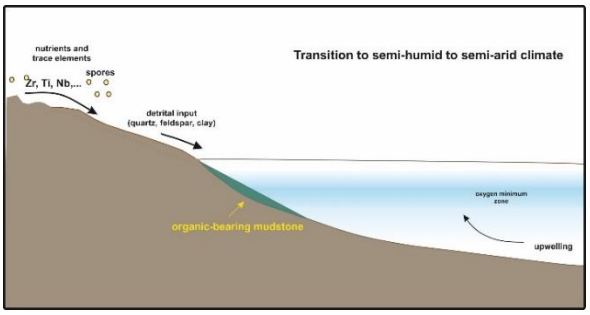

Figure 10. A schematic section of the depositional environment model for the studied mudstones in the shelf setting during the early Cretaceous

5 Conclusions

This study aimed to characterize the depositional environmental conditions controlling organic matter accumulation in lower Cretaceous organic-bearing mudstones exposed around the Çukurca–Karabük area (western Pontides).

The examined mudstones were deposited within a shallow marine shelf-margin to shelf-transition setting influenced by brackish–saline conditions under a semi-humid to semi-arid paleoclimate with moderate chemical weathering.

Proxies for paleoclimate and paleoproductivity indicate that neither factor played a primary role in organic matter enrichment; instead, both likely contributed to dilution of organic matter during deposition.

Redox-sensitive indicators reveal predominantly oxic to suboxic conditions, with episodic oxygen deficiency permitting limited preservation of organic matter. Although such conditions were insufficient to sustain high levels of enrichment, intermittent oxygen restriction appears to have been the main control on organic matter preservation.

Fluctuations in sedimentation rate exerted a dual influence: reduced sedimentation likely enhanced oxidative degradation and decreased preservation efficiency, whereas elevated rates may have limited organic matter accumulation through dilution.

Overall, it is difficult to attribute organic carbon and trace element enrichment to a single controlling mechanism. Instead, multiple oceanographic processes operated concurrently and interacted in a complex manner during deposition.

When considered as a whole, these depositional characteristics indicate that the studied lower Cretaceous mudstones experienced only limited organic matter preservation and enrichment, implying a generally low to moderate hydrocarbon generation potential. Rather than a single dominant mechanism, multiple interacting paleoenvironmental controls collectively constrained source rock quality.

Acknowledgments

The author thanks the Istanbul Technical University (ITU) Geochemistry Research Laboratories (ITU/JAL) team for their valuable contributions to the geochemical analyses.

Conflict of interest

The author declares that there is no conflict of interest.

Similarity rate (iThenticate): 15%

References

[1] D. A. Stow and G. Shanmugam, Sequence of Structures in Fine-Grained Turbidites: Comparison of recent deep-sea and ancient flysch sediments. Sedimentary Geology, 25, 23–42, 1980.

[2] A. C. Aplin and J. H. Macquaker, Mudstone Diversity: Origin and Implications for source, seal, and reservoir properties in petroleum systems. AAPG Bulletin, 95, 2031–2059, 2011. https://doi.org/10.1306/03281110162

[3] Q. Li, S. Wu, D. Xia, X. You, H. Zhang and H. Lu, Major and trace element geochemistry of the lacustrine organic-rich shales from the Upper Triassic Chang 7 Member in the Southwestern Ordos Basin, China: Implications for paleoenvironment and organic matter accumulation. Marine and Petroleum Geology, 111, 852–867, 2020. https://doi.org/10.1016/j.marpetgeo.2019.09.003

[4] A. V. Moradi, A. Sarı and P. Akkaya, Geochemistry of the Miocene oil shale (Hançili Formation) in the Çankırı-Çorum Basin, Central Turkey: Implications for paleoclimate conditions, Source–Area weathering, provenance and tectonic Setting. Sedimentary Geology, 341, 289–303, 2016. https://doi.org/10.1016/j.sedgeo.2016.05.002

[5] B. P. Roser and R. J. Korsch, Determination of Tectonic setting of sandstone-mudstone suites using SiO_2 content and K_2O/Na_2O ratio. The Journal of Geology, 94, 635–650, 1986. https://doi.org/10.1086/629071

[6] S. M. McLennan and S. R. Taylor, Sedimentary rocks and crustal evolution: Tectonic Setting and Secular Trends. The Journal of Geology, 99, 1–21, 1991. https://doi.org/10.1086/629470

[7] H. W. Nesbitt and G. M. Young, Petrogenesis of sediments in the absence of chemical weathering: Effects of abrasion and sorting on bulk composition and mineralogy. Sedimentology, 43, 341–358, 1996. https://doi.org/10.1046/j.1365-3091.1996.d01-12.x

[8] T. Hu, X. Pang, S. Jiang, Q. Wang, T. Xu, K. Lu, C. Huang, Y. Chen and X. Zheng. Impact of paleosalinity, dilution, redox, and paleoproductivity on organic matter enrichment in a saline lacustrine rift basin: A Case Study of Paleogene organic-rich shale in Dongpu depression, Bohai Bay Basin, Eastern China. Energy & Fuels, 32, 5045–5061, 2018. https://doi.org/10.1021/acs.energyfuels.8b00643

[9] X. Wu, L. Xing, Y. Jiang, X. Zhang, R. Xiang and L. Zhou, High-resolution reconstruction of sedimentary organic matter variability during the holocene in the mud area of the Yellow Sea using multiple organic geochemical proxies. Quaternary International, 503, 178–188, 2019. https://doi.org/10.1016/j.quaint.2018.10.012

[10] S. Liu, C. Wu, T. Li and H. Wang, Multiple geochemical proxies controlling the organic matter accumulation of the marine-continental transitional shale: a case study of the upper permian longtan formation, western Guizhou, China. Journal of Natural Gas Science and Engineering, 56, 152–165, 2018. https://doi.org/10.1016/j.jngse.2018.06.007

[11] G. J. Demaison and G. T. Moore, Anoxic environments and oil source bed genesis. Organic Geochemistry, 2, 9–31, 1980. https://doi.org/10.1016/0146-6380(80)90017-0

[12] T. J. Algeo and J. B. Maynard. Trace-element behavior and redox facies in core shales of upper Pennsylvanian Kansas-Type Cyclothems. Chemical Geology, 206, 289–318, 2004. https://doi.org/10.1016/j.chemgeo.2003.12.009

[13] T. J. Algeo and T. W. Lyons, Mo–total organic carbon covariation in modern anoxic marine environments: ımplications for analysis of paleoredox and paleohydrographic conditions. Paleoceanography, 21, 2006. https://doi.org/10.1029/2004PA001112

[14] S. Wang, X. Jin, Q. Bu, L. Jiao and F. Wu, Effects of Dissolved Oxygen Supply Level on Phosphorus Release from Lake Sediments. Colloids and Surfaces A: Physicochemical and Engineering Aspects, 316, 245–252, 2008. https://doi.org/10.1016/j.colsurfa.2007.09.007

[15] Z. Doner, M. Kumral, I.H. Demirel and Q. Hu, Geochemical characteristics of the silurian shales from the central taurides, southern turkey: organic matter accumulation, preservation and depositional environment modeling. Marine and Petroleum Geology, 102, 155–175, 2019. https://doi.org/10.1016/j.marpetgeo.2018.12.042

[16] M. A. Arthur and B. B. Sageman, Marine shales: depositional mechanisms and environments of ancient deposits. Annual Review of Earth and Planetary Sciences, 22, 499–551, 1994.

[17] B. B. Sageman, A. E. Murphy, J. P. Werne and C. A. Ver Straeten, D. J. Hollander, T. W. Lyons, A tale of shales: the relative roles of production, decomposition, and dilution in the accumulation of organic-rich strata, Middle–Upper Devonian, Appalachian Basin. Chemical Geology, 195, 229–273, 2003. https://doi.org/10.1016/S0009-2541(02)00397-2

[18] Tenger, W. Liu, Y. Xu and J. Chen, Comprehensive geochemical ıdentification of highly evolved marine carbonate rocks as hydrocarbon-source rocks as exemplified by the Ordos basin. Science in China Series D, 49, 384–396, 2006. https://doi.org/10.1007/s11430-006-0384-7

[19] Q. Liang, X. Zhang, J. Tian, X. Sun and H. Chang. Geological and geochemical characteristics of marine-continental transitional shale from the lower permian taiyuan formation, taikang uplift, southern north China Basin. Marine and Petroleum Geology, 98, 229–242, 2018. https://doi.org/10.1016/j.marpetgeo.2018.08.027

[20] C. Jin, C. Li, T. J. Algeo, S. Wu, M. Cheng, Z. Zhang and W. Shi, Controls on organic matter accumulation on the Early-Cambrian western Yangtze Platform, south China. Marine and Petroleum Geology, 111, 75–87, 2020. https://doi.org/10.1016/j.marpetgeo.2019.08.005

[21] Y. Nie, X. Fu, J. Liang, H. Wei, Z. Chen, F. Lin, S. Zeng, Y. Wu, Y. Zou and A. Mansour. The Toarcian oceanic anoxic event in a shelf environment (Eastern Tethys): Implications for weathering and redox conditions. Sedimentary Geology, 455, 106476, 2023. https://doi.org/10.1016/j.sedgeo.2023.106476

[22] C. Diessel, R. Boyd, J. Wadsworth, D. Leckie and G. Chalmers, On balanced and unbalanced accommodation/peat accumulation ratios in the Cretaceous coals from Gates Formation, western Canada, and their sequence-stratigraphic significance. International Journal of Coal Geology, 43, 143–186, 2000. https://doi.org/10.1016/S0166-5162(99)00058-0

[23] R. Tyson, Sedimentation rate, dilution, preservation and total organic carbon: some results of a modelling study". Organic Geochemistry, 32, 333–339, 2001. https://doi.org/10.1016/S0146-6380(00)00161-3

[24] X. Ding, G. Liu, M. Zha, Z. Huang, C. Gao, X. Lu, M. Sun, Z. Chen and X. Liuzhuang, Relationship between total organic carbon content and sedimentation rate in ancient lacustrine sediments, a case study of Erlian Basin, northern China. Journal of Geochemical Exploration, 149, 22–29, 2015. https://doi.org/10.1016/j.gexplo.2014.11.004

[25] Y. Chen, Y. Wang, M. Guo, H. Wu, J. Li, W. Wu and J. Zhao, Differential enrichment mechanism of organic matters in the marine-continental transitional shale in northeastern Ordos Basin, China: Control of sedimentary environments. Journal of Natural Gas Science and Engineering, 83, 103625, 2020. https://doi.org/10.1016/j.jngse.2020.103625

[26] D. J. Ross and R. M. Bustin, Investigating the use of sedimentary geochemical proxies for paleoenvironment ınterpretation of thermally mature organic-rich strata: examples from the Devonian–Mississippian Shales, Western Canadian Sedimentary

Basin. Chemical Geology, 260, 1–19, 2009. https://doi.org/10.1016/j.chemgeo.2008.10.027
[27] Y. Nie, X. Fu, X. Liu, H. Wei, S. Zeng, F. Lin, Y. Wan and C. Song, Organic matter accumulation mechanism under global/regional warming: Insight from the Late Barremian Calcareous Shales in the Qiangtang Basin (Tibet). Journal of Asian Earth Sciences, 241, 105456, 2023. https://doi.org/10.1016/j.jseaes.2022.105456
[28] N. Tribovillard, T. J. Algeo, T. Lyons and A. Riboulleau, Trace metals as paleoredox and paleoproductivity proxies: An Update. Chemical Geology, 232, 12–32, 2006. https://doi.org/10.1016/j.chemgeo.2006.02.012
[29] P. Ma, L. Wang, C. Wang, X. Wu and Y. Wei, Organic-Matter accumulation of the lacustrine Lunpola oil shale, central Tibetan Plateau: Controlled by the Paleoclimate, Provenance, and Drainage System. International Journal of Coal Geology, 147, 58–70, 2015. https://doi.org/10.1016/j.coal.2015.06.011
[30] S. Li, Z. Zhou, H. Nie, M. Liu, F. Meng, B., Shen, X. Zhang, X. Zhaodong and S. Zhang, Organic matter accumulation mechanisms in the Wufeng-Longmaxi shales in western Hubei Province, China and paleogeographic implications for the uplift of the Hunan-Hubei Submarine high. International Journal of Coal Geology, 270, 104223, 2023. https://doi.org/10.1016/j.coal.2023.104223
[31] Z. Caineng, Y. Zhi, J. W. Cui, R.K. Zhu, L. H. Hou, S. Z. Tao, X. J. Yuan, S. T. Wu, S. H. Lin and L. Wang, Formation mechanism, geological characteristics and development strategy of nonmarine shale oil in China. Petroleum Exploration and Development, 40 (1), 15–27, 2013. https://doi.org/10.1016/S1876-3804(13)60002-6
[32] F. Hao, H. Zou and Y. Lu, Mechanisms of shale gas storage: implications for shale gas exploration in China. AAPG Bull. 97 (8), 1325–1346, 2013. https://doi.org/10.1306/02141312091
[33] H. Klemme and G. F. Ulmishek, Effective petroleum source rocks of the world: stratigraphic distribution and controlling depositional factors. AAPG Bulletin, 75, 1809–1851, 1991. https://doi.org/10.1306/0C9B2A47-1710-11D7-8645000102C1865D
[34] A. S. Gale, S. Culver and P. Rawson, The Cretaceous world, Biotic response to global change: the last. 145 4-19, 2000. https://doi.org/10.1017/CBO9780511535505.003
[35] W. T. Fratschner, Azdavay, Bartın, Kumluca, Kurucaşile, Ulus bölgelerinde 19-Mayıs- 24 Ekim arasında yapılan etüdlere dair ilk rapor (Rapor No. 1960). MTA Kurumsal Raporu, Ankara, 1952.
[36] W. T. Fratschner, Azdavay sondajlarına ait rapor ve mutalaa (Rapor No. 2408). MTA Kurumsal Raporu, Ankara, 1956.
[37] A. Güven, Stratigraphy and sedimentology of Eocene formations, Karabük Area, Turkey. Ph.D. Thesis, University of Wales, Swansea, 1977.
[38] S. Saner, İ. Taner, Z. Aksoy, M. Siyako and K.A. Bürkan, Karabük-Safranbolu bölgesinin jeolojisi (Rap. No: 1322). TPAO Kurumsal Raporu, Ankara, 1979.
[39] S. Saner, İ. Taner, Z. Aksoy and M. Siyako, K. A. Bürkan, Safranbolu havzasının jeolojik yapısı ve Tersiyer paleocoğrafyası. Türkiye 5. Petrol Kongresi, s. 111- 122, Ankara, 1980.
[40] O. Yılmaz, Daday-Devrekani masifi kuzeydoğu kesimi litostratigrafi birimleri ve tektoniği. Yerbilimleri Dergisi, 5 (5/6), 101-131, 1980.
[41] M. Aydın and Ö. Sahintürk, Cide-Ulus-Azdavay-Araç-Daday-Karadere ve dolaylarının jeolojisi (Rapor No. 1644). TPAO Kurumsal Raporu, Ankara, 1982.
[42] M. Aydın, Ö. Sahintürk and Y. Özçelik, Araç-Daday-Karadere ve dolaylarının jeolojisi ve hidrokarbon olanakları (Rapor No. 1948). TPAO Kurumsal Raporu, Ankara, 1984.
[43] M. Aydın, H. S. Serdar, Ö. Şahintürk, Y. Özçelik, R. Çokugras, İ. Akarsu, A. Üngür ve S. Kasar, Ballıdag-Çangaldagı (Kastamonu) arasındaki bölgenin Jeolojisi. TJK Bülteni, 29, 2, 1-16, 1986.
[44] A. Koçyiğit, Karabük-Safranbolu Tersiyer havzası kuzey kenarının stratigrafisi ve niteliği. TJK. Bülteni, 30-1, 61-69, 1987.
[45] M. Y. Barkurt, E. Bilginer, Ş. Pehlivan, S. Örçen, B. Can, Z. Dağar, C. Bilgi., M. Karabıyıkoğlu ve T. Süer, Kastamonu-Araç güneyinin jeolojisi (Rapor No: 9079), MTA Kurumsal Raporu, Ankara, 1990.
[46] A. S. Derman, Batı Karadeniz bölgesinin Geç Jura-Erken Kretase evrimi. 8. Petrol Kongresi Proceedings, 328-339, 1990.
[47] A. S. Derman, Cretaceous megabreccias and other mass flow deposits in the eastern Ulus Basin, Western Black Sea Region of Turkey. Ph.D. Thesis, METU, The Grad. School of Naturel and Aplied Sciences, Ankara, 1995.
[48] A. S. Derman ve Y. Özçelik, Batı Karadeniz Bölgesi'ndeki Paleozoik birimlerinin stratigrafisi, sedimantolojik özellikleri ve yörenin muhtemel paleocoğrafik evrimi. A. Suat Erk Jeoloji Sempozyumu, Bildiriler, Ankara Üniversitesi Fen Fakültesi Jeoloji Mühendisliği Bölümü, 2-5, 1993.
[49] Y. Özçelik ve A. Çaptuğ, Amasra Dogusu - Cide arasında kalan alanda yapılan saha gözlemleri ve revizyon çalısmaları (Rapor No. 2789). TPAO Kurumsal Raporu, Ankara, 1990.
[50] O. Tüysüz, Geology of the Cretaceous sedimentary basins of the Western Pontides. Geological Journal, 34 (1-2), 75-93, 1999. https://doi.org/10.1002/(SICI)1099-1034(199901/06)34:1/2<75::AID-GJ815>3.0.CO;2-S
[51] Ş. Şen, Karabük-Safranbolu havzasının sedimanter analizi ve bölgedeki diğer çökel havzalarla ilişkileri. Doktora tezi, İstanbul Üniversitesi Fen Bilimleri Enstitüsü, Jeoloji Mühendisliği Anabilim Dalı, 195, İstanbul, 2001.
[52] O. Tüysüz, A. Aksay ve E. Yiğitbaş, Batı Karadeniz bölgesi litostatigrafi birimleri. MTA Stratigrafi Komitesi, Litostatigrafi Birimleri Serisi, 1.92, 2004.

[53] M. F. Uğuz ve M. Sevin, Türkiye Jeoloji Haritaları, Kastamonu F30 Paftası (Rapor No. 144). Maden Tetkik Arama Jeoloji Etüdleri Dairesi yayınları, Ankara, 2011.
[54] A. S. Derman and Y. H. İztan, Results of geochemical analyses of seeps and potential source rocks from Northern Turkey and Turkish Black Sea. AAPG Memoir, 68, 313-330, 1997. https://doi.org/10.1306/M68612C16
[55] O. Harput, Batı Karadeniz Bölgesi tortullarının kaynak kaya ve olgunlaşma yöntemiyle incelenmesi. Doktora tezi, Hacettepe Üniversitesi, Fen Bilimleri Enstitüsü, Ankara, 1997.
[56] B. O. Harput, I. H. Demirel, A. I. Karayigit, M. Aydin, O. Sahinturk and R. M. Bustin, Preliminary hydrocarbon source rock assessment of the Paleozoic and Mesozoic formations of the Western Black Sea region of Turkey. Energy sources, 21(10), 945-956, 1999. https://doi.org/10.1080/00908319950014317
[57] S. Sen, Allochthonous blocks and thrust tectonics effects to petroleum exploration in the Ulus Basin, Western Black Sea of Turkey. In AAPG Annual Convention and Exhibition, 2017.
[58] Ş. Şen, Source rock assessment of the Lower Cretaceous Ulus Formation of NW Turkey: Implication to petroleum exploration. Petroleum Science and Technology, 36(22), 1891-1897, 2018. https://doi.org/10.1080/10916466.2018.1517168
[59] O. Mammadov, Evalution of organic matters and hydrocarbon potential in lower cretaceous mudstones: From Ulus and Kilimli formations, Northwestern part of pontides, Turkey. Yüksek Lisans Tezi, İstanbul Teknik Üniversitesi Fen Bilimleri Enstitüsü, Jeoloji Mühendisliği Ana Bilim Dalı, 121, İstanbul, 2017.
[60] W. Dean, O. Monod, R. Rickards, O. Demir and P. Bultynck, Lower Palaeozoic stratigraphy and palaeontology, Karadere–Zirze area, Pontus mountains, northern Turkey. Geological Magazine, 137, 2000, 555-582. https://doi.org/10.1017/S0016756800004635
[61] N. Özgül, Stratigraphy and some structural features of the İstanbul Paleozoic, Turkish Journal of Earth Sciences, 21 817-866, 2012. https://doi.org/10.3906/yer-1111-6
[62] F. Chen, W. Siebel, M. Satir, M. Terzioğlu and K. Saka, Geochronology of the Karadere basement (NW Turkey) and implications for the geological evolution of the Istanbul zone, International Journal of Earth Sciences. 91 469-481, 2002. https://doi.org/10.1007/s00531-001-0239-6
[63] R. Akdoğan, A. I. Okay, G. Sunal, G. Tari, G. Meinhold and A. R. Kylander-Clark, Provenance of a large Lower Cretaceous turbidite submarine fan complex on the active Laurasian margin: Central Pontides, northern Turkey, Journal of Asian Earth Sciences, 134, 309-329, 2017. http://dx.doi.org/10.1016/j.jseaes.2016.11.028
[64] P. Ayda Ustaömer, R. Mundil and P. R. Renne, U/Pb and Pb/Pb zircon ages for arc-related intrusions of the Bolu Massif (W Pontides, NW Turkey): evidence for Late Precambrian (Cadomian) age, Terra Nova, 17, 215-223, 2005. https://doi:10.1111/j.1365-3121.2005.00594.x
[65] S. Y. Şahin, Y. Güngör, N. Aysal and S. Öngen, Istranca ve İstanbul Zonları (KB Türkiye) İçerisinde Yüzeylenen Granitoyidlerin Jeokimyası ve SHRIMP Zirkon U-Pb Yaşlandırması, içinde: Türkiye Jeoloji Kurultayı, Bidiri Özleri, MTA Ankara, 2009: ss. 598-599.
[66] A. I. Okay, G. Sunal, S. Sherlock, D. Altıner, O. Tüysüz, A. R. Kylander-Clark and M. Aygül, Early Cretaceous sedimentation and orogeny on the active margin of Eurasia: Southern Central Pontides, Turkey. Tectonics, 32, 1247-1271, 2013. https://doi.org/10.1002/tect.20077
[67] E. Timur ve A. Aksay, Türkiye Jeoloji Haritaları, Zonguldak F29 Paftası (Rapor No. 30), Maden Tetkik Arama Jeoloji Etüdleri Dairesi yayınları., Ankara, 2002.
[68] A. Okay, M. Satir and W. Siebel, Pre-Alpide Palaeozoic and Mesozoic orogenic events in the Eastern Mediterranean region, 2006. https://doi.org/10.1144/GSL.MEM.2006.032.01.23
[69] E. Yiğitbaş, A. Elmas and Y. Yïlmaz, Pre-Cenozoic tectono-stratigraphic components of the western pontides and their geological evolution. Geological Journal, 34 55-74, 1999. https://doi.org/10.1002/(SICI)1099-1034(199901/06)34:1/2<55::AID-GJ814>3.0.CO;2-0
[70] A. M. C. Şengör and Y. Yılmaz, Tethyan evolution of Turkey: a plate tectonic approach. Tectonophysics 75, 181–241, 1981. https://doi.org/10.1016/0040-1951(81)90275-4
[71] N. Görür, A. M. C. Şengör, R. Akkök ve Y. Yılmaz, Pontidlerde Neo-Tetis' in kuzey kolunun açılmasına ilişkin sedimentolojik veriler. Türkiye Jeoloji Kurumu Bülteni, 26 (1), 11-20, 1983.
[72] N. Görür, Timing of opening of the Black Sea basin. Tectonophysics, 147 (3-4), 247-262, 1988. https://doi.org/10.1016/0040-1951(88)90189-8
[73] A. I. Okay and A. M. Nikishin, Tectonic evolution of the southern margin of Laurasia in the Black Sea region. International Geology Review, 57(5-8), 1051-1076, 2015. https://doi.org/10.1080/00206814.2015.1010609
[74] İ. Ketin ve A. Gümüş, Sinop-Ayancık güneyinde üçüncü bölgeye dahil sahaların jeolojisi hakkında rapor (2. Kısım: Jura ve Kretase formasyonlarının etüdü), Turkish Petroleum Co. Internal Report, 288 33, 1963.
[75] R. L. Cullers, The geochemistry of shales, siltstones and sandstones of Pennsylvanian–Permian age, Colorado, USA: implications for provenance and metamorphic studies. Lithos, 51 181-203, 2000. https://doi.org/10.1016/S0301-9268(00)00090-5
[76] J. Armstrong-Altrin and S. P. Verma, Critical evaluation of six tectonic setting discrimination diagrams using geochemical data of Neogene

sediments from known tectonic settings. Sedimentary Geology. 177, 115-129, 2005. https://doi.org/10.1016/j.sedgeo.2005.02.004

[77] E. A. Abou El-Anwar, Mineralogical, petrographical, geochemical, diageneses and provenance of the cretaceous black shales, Duwi formation at Quseir-Safaga, Red Sea, Egypt. Egyptian Journal of Petroleum, 26, 915-926, 2017. https://doi.org/10.1016/j.ejpe.2016.06.005

[78] S. McLennan, S. Hemming, D. McDaniel and G. Hanson, Geochemical approaches to sedimentation, provenance, and tectonics, 1993. https://doi.org/10.1130/SPE284-p21

[79] K.-I. Hayashi, H. Fujisawa, H. D. Holland and H. Ohmoto, Geochemistry of~ 1.9 Ga sedimentary rocks from northeastern Labrador, Canada. Geochimica et Cosmochimica Acta, 61 4115-4137, 1997. https://doi.org/10.1016/S0016-7037(97)00214-7

[80] S. Wang, X. Huang and J. Tuo, Evolutional characteristics and their paleoclimate significance of trace elements in the Hetaoyuan Formation, Biyang depression. Acta Sedimentologica Sinica, 15, 65-70, 1997.

[81] A. K. Adegoke, W. H. Abdullah, M. H. Hakimi and B. M. S. Yandoka, Geochemical characterisation and organic matter enrichment of Upper Cretaceous Gongila shales from Chad (Bornu) Basin, northeastern Nigeria: Bioproductivity versus anoxia conditions. Journal of Petroleum Science and Engineering, 135 73-87, 2015. http://dx.doi.org/10.1016/j.petrol.2015.08.012

[82] J. Jia, Z. Liu, A. Bechtel, S. A. Strobl and P. Sun, Tectonic and climate control of oil shale deposition in the Upper Cretaceous Qingshankou Formation (Songliao Basin, NE China). International Journal of Earth Sciences, 102 1717-1734, 2013. https://doi.org/10.1007/s00531-013-0903-7

[83] H. Chang, Z. An, F. Wu, Z. Jin, W. Liu and Y. Song, A Rb/Sr record of the weathering response to environmental changes in westerly winds across the Tarim Basin in the late Miocene to the early Pleistocene. Palaeogeography, Palaeoclimatology, Palaeoecology, 386 364-373, 2013. https://doi.org/10.1016/j.palaeo.2013.06.006

[84] D. K. Roy and B. P. Roser, Climatic control on the composition of Carboniferous–Permian Gondwana sediments, Khalaspir basin, Bangladesh. Gondwana Research, 23 1163-1171, 2013. https://doi.org/10.1016/j.gr.2012.07.006

[85] J. Cao, M. Wu, Y. Chen, K. Hu, L. Bian, L. Wang and Y. Zhang, Trace and rare earth element geochemistry of Jurassic mudstones in the northern Qaidam Basin, northwest China. Geochemistry, 72, 245-252, 2012. https://doi.org/10.1016/j.chemer.2011.12.002

[86] H. W. Nesbitt and G. M. Young, Formation and diagenesis of weathering profiles. The Journal of Geology, 97, 129-147, 1989. https://doi.org/10.1086/629290

[87] H. W. Nesbitt and G. M. Young, Early Proterozoic climates and plate motions inferred from major element chemistry of lutites. Nature, 299 715-717, 1982.

[88] W. He, S. Tao, L. Hai, R. Tao, X. Wei and L. Wang, Geochemistry of the tanshan oil shale in jurassic coal measures, western ordos basin: implications for sedimentary environment and organic matter accumulation. Energies, 15 8535, 2022. https://doi.org/10.3390/en15228535

[89] L. Zhao, Y. Li, C. Zou, S. Zhao and C. Wu, Paleoenvironmental characteristics and organic matter enrichment mechanisms of the upper Ordovician-lower Silurian organic-rich black shales in the Yangtze foreland basin, South China. Frontiers in Earth Science, 11 1237495, 2023. https://doi.org/10.3389/feart.2023.1237495

[90] C. M. Fedo, G. M. Young and H. W. Nesbitt, Paleoclimatic control on the composition of the Paleoproterozoic Serpent Formation, Huronian Supergroup, Canada: a greenhouse to icehouse transition. Precambrian Research, 86 201-223, 1997. https://doi.org/10.1016/S0301-9268(97)00049-1

[91] H. W. Nesbitt and G. M. Young, Prediction of some weathering trends of plutonic and volcanic rocks based on thermodynamic and kinetic considerations, Geochimica et cosmochimica acta, 48, 1523-1534, 1984. https://doi.org/10.1016/0016-7037(84)90408-3

[92] C. Kasanzu, M. A. Maboko and S. Manya, Geochemistry of fine-grained clastic sedimentary rocks of the Neoproterozoic Ikorongo Group, NE Tanzania: Implications for provenance and source rock weathering. Precambrian Research, 164, 201-213, 2008. https://doi.org/10.1016/j.precamres.2008.04.007

[93] S. Han, Y. Zhang, J. Huang, Y. Rui and Z. Tang, Elemental geochemical characterization of sedimentary conditions and organic matter enrichment for Lower Cambrian shale formations in Northern Guizhou, South China. Minerals, 10, 793, 2020. https://doi.org/10.3390/min10090793

[94] S.R. Taylor and S.M. McLennan, The continental crust: its composition and evolution, 1985.

[95] R. Cox, D.R. Lowe and R. Cullers, The influence of sediment recycling and basement composition on evolution of mudrock chemistry in the southwestern United States. Geochimica et Cosmochimica Acta, 59 2919-2940, 1995. https://doi.org/10.1016/0016-7037(95)00185-9

[96] L. Feng, X. Chu and Q. Zhang, CIA (chemical index of alteration) and its applications in the Neoproterozoic clastic rocks, Earth Science Frontiers, 10, 539-544, 2003.

[97] B. Zhang, P. B. Wignall, S. Yao, W. Hu and B. Liu, Collapsed upwelling and intensified euxinia in response to climate warming during the Capitanian (Middle Permian) mass extinction. Gondwana Research. 89, 31-46, 2021. https://doi.org/10.1016/j.gr.2020.09.003

[98] D. Yan, D. Chen, Q. Wang and J. Wang, Large-scale climatic fluctuations in the latest Ordovician on the Yangtze block, south China. Geology, 38 599-602, 2010. https://doi.org/10.1130/G30961.1

[99] S. Zeng, J. Wang, X. Fu, W. Chen, X. Feng, D. Wang, C. Song and Z. Wang, Geochemical characteristics, redox conditions, and organic matter accumulation of marine oil shale from the Changliang Mountain area, northern Tibet, China. Marine and Petroleum Geology, 64, 203-221, 2015. https://doi.org/10.1016/j.marpetgeo.2015.02.031

[100] P. Wignall and R. Newton, Black shales on the basin margin: a model based on examples from the Upper Jurassic of the Boulonnais, northern France, Sedimentary Geology, 144, 335-356, 2001. https://doi.org/10.1016/S0037-0738(01)00125-7

[101] D. J. Wronkiewicz and K. C. Condie, Geochemistry of Archean shales from the Witwatersrand Supergroup, South Africa: source-area weathering and provenance, Geochimica et Cosmochimica Acta. 51, 2401-2416, 1987. https://doi.org/10.1016/0016-7037(87)90293-6

[102] R. V. Tyson and T. H. Pearson, Modern and ancient continental shelf anoxia: an overview, Geological Society, London, Special Publications, 58, 1-24, 1991. https://doi.org/10.1144/GSL.SP.1991.058.01.01

[103] T. J. Algeo and C. Li, Redox classification and calibration of redox thresholds in sedimentary systems. Geochimica et Cosmochimica Acta, 287, 8-26, 2020. https://doi.org/10.1016/j.gca.2020.01.055

[104] B. Jones, D. A. Manning, Comparison of geochemical indices used for the interpretation of palaeoredox conditions in ancient mudstones. Chemical Geology, 111, 111-129, 1994. https://doi.org/10.1016/0009-2541(94)90085-X

[105] T. J. Algeo, K. Kuwahara, H. Sano, S. Bates, T. Lyons, E. Elswick, L. Hinnov, B. Ellwood, J. Moser and J. B. Maynard, Spatial variation in sediment fluxes, redox conditions, and productivity in the Permian–Triassic Panthalassic Ocean. Palaeogeography, Palaeoclimatology, Palaeoecology, 308, 65-83, 2011. http://dx.doi.org/10.1016/j.palaeo.2010.07.007

[106] S. Zhang, C. Liu, Z. Fan, H. Liang, J. Gao, H. Song, W. Dang, L. Zhang and Y. Gao, Paleoenvironmental Conditions and Shale Oil Potential of the Carboniferous Ha'erjiawu Formation in the Santanghu Basin, NW China. Processes, 11, 2209, 2023. https://doi.org/10.3390/pr11072209

[107] T. J. Algeo and J. Liu, A re-assessment of elemental proxies for paleoredox analysis, 2020. https://doi.org/10.1016/j.chemgeo.2020.119549

[108] P. B. Wignall and R. J. Twitchett, Oceanic anoxia and the end Permian mass extinction. Science, 272, 1155-1158, 1996. https://doi.org/10.1126/science.272.5265.1155

[109] H. Kimura and Y. Watanabe, Oceanic anoxia at the Precambrian-Cambrian boundary. Geology, 29, 995-998, 2001. https://doi.org/10.1130/0091-7613(2001)029<0995:OAATPC>2.0.CO;2

[110] C. Scott and T. W. Lyons, Contrasting molybdenum cycling and isotopic properties in euxinic versus non-euxinic sediments and sedimentary rocks: Refining the paleoproxies, Chemical Geology, 324, 19-27, 2012. https://doi.org/10.1016/j.chemgeo.2012.05.012

[111] T. J. Algeo and N. Tribovillard, Environmental analysis of paleoceanographic systems based on molybdenum–uranium covariation. Chemical Geology, 268, 211-225, 2009. https://doi.org/10.1016/j.chemgeo.2009.09.001

[112] N.-P. Tribovillard, A. Desprairies, E. Lallier-Vergès, P. Bertrand, N. Moureau, A. Ramdani and L. Ramanampisoa, Geochemical study of organic-matter rich cycles from the Kimmeridge Clay Formation of Yorkshire (UK): productivity versus anoxia. Palaeogeography, Palaeoclimatology, Palaeoecology. 108, 165-181, 1994. https://doi.org/10.1016/0031-0182(94)90028-0

[113] T. J. Algeo and E. Ingall, Sedimentary Corg: P ratios, paleocean ventilation, and Phanerozoic atmospheric pO2. Palaeogeography, Palaeoclimatology, Palaeoecology, 256 130-155, 2007. http://dx.doi.org/10.1016/j.palaeo.2007.02.029

[114] S. D. Schoepfer, J. Shen, H. Wei, R. V. Tyson, E. Ingall and T. J. Algeo, Total organic carbon, organic phosphorus, and biogenic barium fluxes as proxies for paleomarine productivity, Earth-Science Reviews, 149, 23-52, 2015. https://doi.org/10.1016/j.earscirev.2014.08.017

[115] Y. Zhang, C. Lyu, X. Gao, Z. Dang, Z. Sun, Q. Zhou and G. Chen, Geochemical Characteristics and Organic Matter Accumulation of Wufeng-Longmaxi Shales in the Southeast of the Sichuan Basin of South China. Geofluids, 7360065, 2022. https://doi.org/10.1155/2022/7360065

[116] A. Mansour and M. Wagreich, Earth system changes during the cooling greenhouse phase of the Late Cretaceous: Coniacian-Santonian OAE3 subevents and fundamental variations in organic carbon deposition. Earth-Science Reviews, 229, 104022, 2022. https://doi.org/10.1016/j.earscirev.2022.104022

[117] H. Dill, Metallogenesis of early Paleozoic graptolite shales from the Graefenthal Horst (northern Bavaria-Federal Republic of Germany). Economic Geology, 81, 889-903, 1986. https://doi.org/10.2113/gsecongeo.81.4.889

[118] X. Tang, J. Zhang, Y. Liu, C. Yang, Q. Chen, W. Dang and P. Zhao, Geochemistry of organic matter and elements of black shale during weathering in Northern Guizhou, Southwestern China: Their mobilization and inter-connection. Geochemistry, 78, 140-151, 2018. https://doi.org/10.1016/j.chemer.2017.08.002

[119] H. Cao, W. Guo, X. Shan, L. Ma and P. Sun, Paleolimnological environments and organic accumulation of the Nenjiang formation in the

southeastern Songliao Basin, China., Oil Shale, 32, 2015. https://doi.org/10.3176/oil.2015.1.02

[120] S. Tao, Y. Xu, D. Tang, H. Xu, S. Li, S. Chen, W. Liu, Y. Cui and M. Gou, Geochemistry of the Shitoumei oil shale in the Santanghu Basin, Northwest China: Implications for paleoclimate conditions, weathering, provenance and tectonic setting. International Journal of Coal Geology, 184 42-56, 2017. https://doi.org/10.1016/j.coal.2017.11.007

[121] W. Wei and T. J. Algeo, Elemental proxies for paleosalinity analysis of ancient shales and mudrocks, Geochimica et Cosmochimica Acta. 287, 341-366, 2020. https://doi.org/10.1016/j.gca.2019.06.034

[122] F. Campbell and G. Williams, Chemical composition of shales of Mannville group (lower Cretaceous) of central Alberta, Canada, AAPG Bulletin. 49, 81-87, 1965. https://doi.org/10.1306/A66334EA-16C0-11D7-8645000102C1865D

[123] X. Zhang, Z. Gao, T. Fan, J. Xue, W. Li, H. Zhang and F. Cao, Element geochemical characteristics, provenance attributes, and paleosedimentary environment of the Paleogene strata in the Lenghu area, northwestern Qaidam Basin, Journal of Petroleum Science and Engineering, 195 ,107750, 2020. https://doi.org/10.1016/j.petrol.2020.107750

[124] M. N. Remírez and T. J. Algeo, Paleosalinity determination in ancient epicontinental seas: A case study of the T-OAE in the Cleveland Basin (UK). Earth-Science Reviews, 201 103072, 2020. https://doi.org/10.1016/j.earscirev.2019.103072

[125] L. Tang, Y. Song, S. Jiang, Z. Jiang, Z. Li, Y. Yang, X. Li and L. Xiao, Organic matter accumulation of the Wufeng-Longmaxi shales in southern Sichuan Basin: Evidence and insight from volcanism. Marine and Petroleum Geology, 120, 104564, 2020. https://doi.org/10.1016/j.marpetgeo.2020.104564

[126] J. Dymond, E. Suess and M. Lyle, Barium in deep-sea sediment: A geochemical proxy for paleoproductivity. Paleoceanography, 7, 163-181, 1992. https://doi.org/10.1029/92PA00181

[127] R. W. Murray and M. Leinen, Chemical transport to the seafloor of the equatorial Pacific Ocean across a latitudinal transect at 135 W: tracking sedimentary major, trace, and rare earth element fluxes at the Equator and the Intertropical Convergence Zone. Geochimica et Cosmochimica Acta, 57, 4141-4163, 1993. https://doi.org/10.1029/93PA02195

[128] D. Yan, H. Wang, Q. Fu, Z. Chen, J. He and Z. Gao, Organic matter accumulation of Late Ordovician sediments in North Guizhou Province, China: Sulfur isotope and trace element evidences. Marine and Petroleum Geology, 59, 348-358, 2015. https://doi.org/10.1016/j.marpetgeo.2014.09.017

[129] D. Piper and R. Perkins, A modern vs. Permian black shale—the hydrography, primary productivity, and water-column chemistry of deposition. Chemical Geology. 206, 177-197, 2004. https://doi.org/10.1016/j.chemgeo.2003.12.006

[130] A. E. Murphy, B. B. Sageman, D. J. Hollander, T. W. Lyons and C. E. Brett, Black shale deposition and faunal overturn in the Devonian Appalachian Basin: Clastic starvation, seasonal water-column mixing, and efficient biolimiting nutrient recycling. Paleoceanography, 15 280-291, 2000. https://doi.org/10.1029/1999PA000445

[131] L. Chen, M. Xiong, X. Tan, X. Chen, J. Zheng, Y. Yang, C. Jing and G. Wang, Coupling mechanism between sea level changes and pore heterogeneity of marine shale reservoirs driven by astronomical orbital cycles: Lower Silurian Longmaxi shale in the Upper Yangtze area, South China. Marine and Petroleum Geology, 160, 106590, 2024. https://doi.org/10.1016/j.marpetgeo.2023.106590

[132] M. Reolid, J. M. Molina, L. M. Nieto and F. J. Rodríguez-Tovar, The Toarcian oceanic anoxic event in the South Iberian Palaeomargin, Springer, 2018.

[133] D. E. Ruhlin and R. M. Owen, The rare earth element geochemistry of hydrothermal sediments from the East Pacific Rise: Examination of a seawater scavenging mechanism. Geochimica et Cosmochimica Acta. 50, 393-400, 1986. https://doi.org/10.1016/0016-7037(86)90192-4

[134] H. C. Jenkyns, Geochemistry of oceanic anoxic events. Geochemistry, Geophysics, Geosystems, 11, 2010. https://doi.org/10.1029/2009GC002788

[135] F. Yang, G.-L. Zhang, J.-L. Yang, D.-C. Li, Y.-G. Zhao, F. Liu, R.-M. Yang and F. Yang, Organic matter controls of soil water retention in an alpine grassland and its significance for hydrological processes. Journal of Hydrology, 519, 3086-3093, 2014. https://doi.org/10.1016/j.jhydrol.2014.10.054

[136] M. Usman, M. Ardila-Sanchez, E. Idiz, I. S. Abu-Mahfouz, F. van Buchem and V. Vahrenkamp, Organic and inorganic geochemical cyclicity of a Maastrichtian oceanic open-shelf carbonate source rock, Scientific Reports, 15, 15993, 2025. https://doi.org/10.1038/s41598-025-99832-w

[137] N. P. Kozik, A Tour of Ordovician Paleoredox Conditions: A Primary Driver for Ancient Biodiversity. The Florida State University, 2022.

[138] D. Muñoz-López, A. Koeshidayatullah, T. Bover-Arnal, A. Herlambang, J. D. Martín-Martín, R. Salas, J. D. Humphrey and K. Al-Ramadan, Isotope record of Aptian third-order sea-level trends in platform margin carbonates: implications for sequence stratigraphic analysis. Journal of Sedimentary Research, 95, 417-433, 2025. https://doi.org/10.2110/jsr.2024.124

[139] S. Westermann, M. Stein, V. Matera, N. Fiet, D. Fleitmann, T. Adatte and K.B. Föllmi, Rapid changes in the redox conditions of the western Tethys Ocean during the early Aptian oceanic anoxic event, Geochimica et Cosmochimica Acta, 121, 467-486, 2013. https://doi.org/10.1016/j.gca.2013.07.023